Available online at www.sciencedirect.com
ScienceDirect
Coordination Chemistry Reviews 251 (2007) 2292–2310
COORDINATION CHEMISTRY REVIEWS
www.elsevier.com/locate/ccr

Review

Non-covalent binding of luminescent transition metal polypyridine complexes to avidin, indole-binding proteins and estrogen receptors

Kenneth Kam-Wing Lo [a,*], Keith Hing-Kit Tsang [a], Ka-Shing Sze [a], Chi-Keung Chung [a], Terence Kwok-Ming Lee [a], Kenneth Yin Zhang [a], Wai-Ki Hui [a], Chi-Kwan Li [a], Jason Shing-Yip Lau [a], Dominic Chun-Ming Ng [a], Nianyong Zhu [b]

[a] *Department of Biology and Chemistry, City University of Hong Kong, Tat Chee Avenue, Kowloon, Hong Kong, PR China*
[b] *Department of Chemistry, The University of Hong Kong, Pokfulam Road, Hong Kong, PR China*

Received 27 September 2006; accepted 8 December 2006
Available online 14 December 2006

Contents

Abstract

A number of luminescent transition metal complexes possess rich photophysical and photochemical properties that allow them to serve as useful labels and probes for biological molecules. This article describes the current trend in this area of research, with emphasis on our recent work on luminescent rhenium(I), iridium(III) and ruthenium(II) polypyridine complexes as non-covalent probes for avidin, indole-binding proteins and estrogen receptors. We focus on the molecular design, photophysical properties and biomolecule-binding behaviour of these systems; different approaches to enhancing the detection sensitivity are also discussed.

Keywords: Avidin; Biological probes; Biotin; Estrogen receptors; Indole-binding proteins; Luminescence

Abbreviations: An-Av, anthracene-avidin; bpy, 2,2′-bipyridine; bpy-CONH-C_2H_4-indole, 4-(*N*-(2-indol-3-ylethyl)amido)-4′-methyl-2,2′-bipyridine; bpy-CONH-C_5H_{10}-CONH-C_2H_4-indole, 4-(*N*-(6-*N*-(2-indol-3-ylethyl)hexanamidyl)amido)-4′-methyl-2,2′-bipyridine; bpy-CONH-Et, 4-(*N*-(ethyl)amido)-4′-methyl-2,2′-bipyridine; BSA, bovine serum albumin; DNA, deoxyribonucleic acid; dppn, benzo[*i*]dipyrido[3,2-*a*:2′,3′-*c*]phenazine; dppz, dipyrido[3,2-*a*:2′,3′-*c*]phenazine; dppzB, 11-((2-biotinamido)ethyl)amidodipyrido[3,2-*a*:2′,3′-*c*]phenazine; dpq, dipyrido[3,2-*f*:2′,3′-*h*]quinoxaline; dpqa, 2-(*n*-butylamido)dipyrido[3,2-*f*:2′,3′-*h*]quinoxaline; dpqB, 2-((2-biotinamido)ethyl)amidodipyrido[3,2-*f*:2′,3′-*h*]quinoxaline; dpq-C6-B, 2-((6-biotinamido)hexyl)amidodipyrido[3,2-*f*:2′,3′-*h*]quinoxaline; ERs, estrogen receptors; HABA, 4′-hydroxyazobenzene-2-carboxylic acid; Hppy, 2-phenylpyridine; IL, intraligand; Me_2-phen, 2,9-dimethyl-1,10-phenanthroline; Me_4-phen, 3,4,7,8-tetramethyl-1,10-phenanthroline; MLCT, metal-to-ligand charge-transfer; NHS, *N*-hydroxysuccinimide; PEG_{1900}, poly(ethylene glycol)$_{1900}$; phen, 1,10-phenanthroline; Ph_2-phen, 4,7-diphenyl-1,10-phenanthroline; py, pyridine; py-C6-est, 4-(*N*-(6-(4-(17α-ethynylestradiolyl)phenylamido)hexanoyl)aminomethyl)pyridine; py-4-CH_2-NH-biotin, 4-(biotinamidomethyl)pyridine; py-4-CH_2-NH-C6-NH-biotin, 4-(*N*-((6-biotinamido)hexanoyl)aminomethyl)pyridine; py-3-CONH-C_2H_4-indole, *N*-(3-pyridoyl)tryptamine; py-3-CONH-C_5H_{10}-CONH-C_2H_4-indole, *N*-(*N*-(3-pyridoyl)-6-aminohexanoyl)tryptamine; py-3-CONH-C2-NH-biotin, 3-(*N*-((2-biotinamido)ethyl)amido)pyridine; py-3-CONH-Et, *N*-ethyl-(3-pyridyl)formamide; py-est, 4-(17α-ethynylestradiolyl)pyridine; RET, resonance-energy transfer; SCE, saturated calomel electrode; TPase, tryptophanase

* Corresponding author. Tel.: +852 2788 7231; fax: +852 2788 7406.
E-mail address: bhkenlo@cityu.edu.hk (K.K.-W. Lo).

0010-8545/$ – see front matter © 2006 Elsevier B.V. All rights reserved.
doi:10.1016/j.ccr.2006.12.005

1. Introduction

Many transition metal polypyridine complexes display intense and long-lived emission in the visible region and possess rich photoredox behaviour [1–6]. These properties enable them to serve as useful labels and probes for biomolecules such as DNA and proteins. Since earlier work on introduction of metal complexes to oligonucleotides [7–9], there has been much interest in this area of research. DNA labels derived from luminescent transition metal complexes can be introduced before the oligonucleotides are synthesised or they can react with oligonucleotides that have been modified with a primary amine or sulfhydryl moiety. On the basis of these methods, luminescent ruthenium(II) [10–16], osmium(II) [13,14,17], rhenium(I) [18–20] and iridium(III) [21] polypyridine complexes have been utilised as covalent labels for oligonucleotides. Some of these complexes are highly oxidising in the excited state, rendering them promising candidates as DNA photocleavage agents [16]. Additionally, transition metal complexes with extended planar polypyridine ligands have been designed as DNA metallointercalators; a number of these systems show substantial changes of emission properties upon binding to DNA molecules [22–25].

Different strategies have been used to attach transition metal complexes to proteins; for example, the imidazole of a histidine residue can act as a ligand for various metal centres; cytochrome *c*, azurin and their genetic variants have been conjugated with photoactive ruthenium(II) [26–28] and rhenium(I) [29–31] complexes to investigate long-range electron-transfer. In addition, the lysine residue of a protein molecule can be modified by a bipyridine ligand containing an NHS ester, and metal precursor complexes can react with this ligand to form luminescent bioconjugates [32]. Alternatively, luminescent transition metal complexes carrying reactive functional groups such as NHS ester [33–36], isothiocyanate [18,21,33,37–39] and aldehyde [40–42] can be used to target the amine groups of lysine residues and the N-terminal of proteins [43]; luminescent complexes containing a maleimide [19,44] or iodoacetamide [38,45] group can react with the sulfhydryl group of a cysteine residue [43]. Labelling of various proteins by these strategies has led to the design of new bioassays [33–36,38,40,45].

The development of non-covalent probes for proteins commonly relies on hydrophobic interactions between the metal complexes and the substrate-binding sites of proteins; for example, ruthenium(II) [46] and rhenium(I) [47] diimine adamantane and imidazole complexes containing a perfluorobiphenyl linker bind tightly to cytochrome P450cam and nitric oxide synthase. The binding results from hydrophobic interactions between the complexes and the substrate access channel of the protein [46] and in the case of the rhenium complexes, the ligation of imidazole to the haem of nitric oxide synthase [47]. In another study, a PEG_{1900} substituent has been linked to a cyclometallated platinum(II) complex to yield a luminescent polymer that can function as a probe for proteins [48].

This review article describes our recent work on the design of luminescent transition metal polypyridine complexes as specific biological probes. These probes contain a biologically important substrate as the recognition element and a luminescent metal complex as the reporting unit. Emphasis is placed on the non-covalent binding interactions of these complexes to three different types of biomolecules: avidin, indole-binding proteins and estrogen receptors. For some of our earlier work on luminescent transition metal biotin complexes, readers are referred to our recent review article [49].

2. Biotin complexes

Avidin (MW = 68 kDa) is a glycoprotein isolated from chicken egg white. It has four identical subunits, each containing 128 amino acid residues [50,51]. Tetrameric avidin can bind up to four biotin molecules (Vitamin H) with an exceptionally high affinity (K_d = ca. 10^{-15} M) and the binding is very stable over a wide range of pH, temperature and in various organic solvents [50]. The X-ray structure of avidin reveals that the size of the tetrameric avidin molecule is ca. 56 Å × 50 Å × 40 Å and the four identical subunits are arranged in a quaternary structure which positions the two pairs of the binding sites on opposite sides of the protein [52–54]. The biotin-binding sites of avidin are located at ca. 9 Å below the surface of the avidin molecule and contain both hydrophobic and polar residues for the recognition of biotin [52–54].

The avidin–biotin system has been widely employed in many bioanalytical applications [50,51,55–57]. In a heterogeneous assay, biotinylated biomolecules immobilised on a solid phase can be detected by avidin that has been conjugated with reporters such as fluorescent compounds or enzymes. Actually, many organic fluorophores have been equipped with a biotin moiety to serve as probes for avidin [58–61]. Upon binding to the protein in solution, most of the biotin-fluorophore conjugates experience fluorescence quenching due to RET, or specifically, homotransfer [62]. Since the fluorescence originates from a singlet excited state, the Stokes' shifts of these compounds are usually small, and the overlap integrals are generally large. Thus, when the organic fluorophores come to close proximity, effective RET occurs, leading to substantial emission self-quenching [58–60]. For example, the fluorescence intensity of biotin-4-fluorescein is strongly quenched after binding to avidin [58,59]. The affinity is high enough to achieve stoichiometric ligand binding at low protein concentration and the association rate is fast enough for rapid binding at nanomolar concentration. The fluorescence intensity of another biotin-BODIPY conjugate is also quenched upon binding to avidin [60]. The extent of the decrease in fluorescence intensity has been correlated to the concentration of avidin. Although most biotin-fluorophore conjugates experience avidin-induced fluorescence quenching, a biotin-Cy3 conjugate with a PEG_{1900} spacer-arm has been designed to probe avidin [61]; the use of such a linker can minimise dye–dye and protein–dye interactions and thus reduce self-quenching.

Various biotin compounds containing a reporter or functional unit such as a transition metal complex have been developed; for example, a tricarbonyl(η^5-cyclopentadienyl)manganese biotin compound has been used as an IR-active tracer in competitive bioassays [63]. Redox-active ferrocene-biotin conjugates containing a poly(ethylene oxide) chain have been designed as electrochemical sensors for avidin [64]. Another biotiny-

lated iron(II) diimine complex $[Fe(N{-}N)_3]^{2+}$ has been used as a redox-active biotin-bridge for the immobilisation of avidin layers on an electrode surface [65]. Additionally, a nickel(salen)-biotin conjugate that can couple with highly accessible guanine residues in DNA has been reported [66]. Incubation of a model oligonucleotide with this conjugate yielded a high molecular weight DNA adduct that can be isolated using avidin. Recently, biotin has been attached to ruthenium(II) polypyridine complexes and the binding to avidin has been studied by spectroscopic titrations [67,68]. Specifically, the binding of diastereo pure ruthenium(II) bipyridine biotin complexes to avidin and streptavidin has been examined in detail by CD titrations [67]. The results suggested strong cooperativity between the first and the second binding events and a pronounced difference in affinity between avidin and streptavidin for the cationic ruthenium(II) complex due to the high positive charge of avidin. Additionally, modest enantiodiscrimination with avidin as the host has been observed. In another interesting study, an organometallic ruthenium(II) biotin complex has been incorporated into avidin or streptavidin to give artificial metalloenzymes for the reduction of ketones by transfer hydrogenation [69]. Up to 94% (*R*) enantiomeric excess for the reduction of *p*-methylacetophenone has been achieved.

Since avidin has four biotin-binding sites, theoretically, immobilised biotinylated biomolecules can be recognised by biotin-reporter conjugates when avidin is used as a bridge [43]. While the use of biotin–fluorophores is limited due to self-quenching, for the purpose of a recognition assay, luminescent transition metal complexes could be used as markers or affinity labels in view of their characteristic photophysical properties [23,70–75]. The insignificant overlap integrals prevent them from self-quenching when the complexes bind to avidin. In view of this, we have synthesised a number of luminescent rhenium(I) [76,77], iridium(III) [78,79] and ruthenium(II) [80] biotin complexes and studied their binding to avidin [49]. Our key results are summarised as follows. (1) All the complexes exhibit increased emission intensities and lifetimes upon binding to avidin. (2) More hydrophobic complexes show higher avidin-induced emission enhancement factors (I/I_o). (3) Various quenchers (energy and electron acceptors) have been used in the development of new bioassays. To increase the sensitivity of detection, it is desirable to maximise the avidin-induced emission enhancement factors. One strategy involves the identification of a system that inherently shows very weak emission in aqueous buffer, but intense emission in more hydrophobic media. In view of the interesting DNA-induced emission of a ruthenium(II) amidodipyrido[3,2-*f*:2′,3′-*h*]quinoxaline complex reported by Kelly and co-workers [81], we anticipate that related rhenium(I) amidodipyridoquinoxaline complexes are very promising candidates as sensitive biological probes. Luminescent rhenium(I) amidodipyridoquinoxaline biotin complexes $[Re(dpqa)(CO)_3(L)](PF_6)$ (L = py-4-CH_2-NH-biotin (**1**), py-3-CONH-C2-NH-biotin (**2**), py-4-CH_2-NH-C6-NH-biotin (**3**)) and their biotin-free counterpart $[Re(dpqa)(CO)_3(py)](PF_6)$ (**4**) have been synthesised and characterised [82]. Their structures and those of the dpq analogues [77] are shown in Fig. 1. Excitation of complexes **1**–**4** in fluid solutions at 298 K results

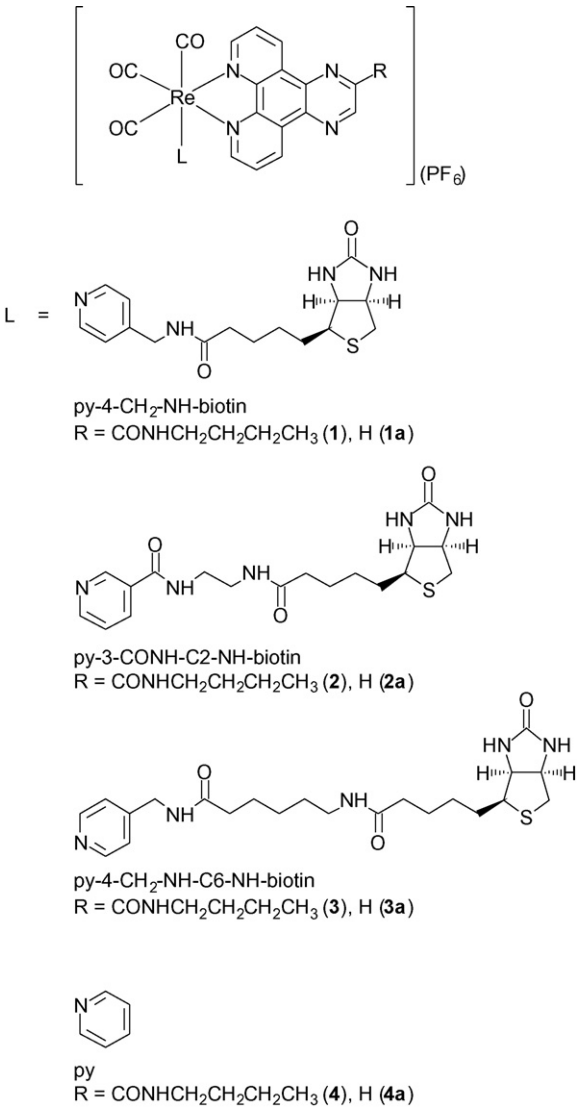

Fig. 1. Structures of complexes **1**–**4** and **1a**–**4a**. Reproduced from Ref. [82], with permission of The American Chemical Society.

in green to yellow ^{3}MLCT ($d\pi(Re) \rightarrow \pi^*(dpqa)$) luminescence [83,84]. The photophysical data of complexes **1**–**4** and their dpq analogues **1a**–**4a** are summarised in Table 1. The emission of complexes **1**–**4** occurs at slightly lower energy than that of their dpq analogues **1a**–**4a** (Table 1). It is obvious that the electron-withdrawing amide substituent of the dpqa ligand stabilises the empty π^* orbitals of the diimine ligand and thus lowers the ^{3}MLCT transition energy of the complexes. Whilst complexes **1**–**4** in relatively non-polar CH_2Cl_2 show emission quantum yields that are comparable to their dpq counterparts (Table 1) and other rhenium(I) polypyridine complexes [83,84], their quantum yields in more polar aqueous buffer are extremely small (ca. 10^{-3}) (Table 1). In other words, they undergo very significant reduction in emission quantum yields upon changing the solvent from CH_2Cl_2 to aqueous buffer ($\Phi_{buffer} : \Phi_{CH_2Cl_2} = 1.8\%$). The corresponding changes for complexes **1a**–**4a** are milder ($\Phi_{buffer} : \Phi_{CH_2Cl_2} = 14.4\%$). The substantial decrease in emission quantum yields for complexes **1**–**4** is ascribed to both the

Table 1
Photophysical data of complexes **1**–**4** and **1a**–**4a**

Complex	Medium (T (K))	λ_{em} (nm[a])	τ_o (μs[a])	Φ_{em}[a]	I (τ (μs))[b,c]	I (τ (μs))[b,d]	I (τ (μs))[b,e]
1	CH_2Cl_2 (298)	553	0.92	0.19	1.00 (0.19)	8.05 (0.34)	0.96 (0.21)
	CH_3CN (298)	573	0.34	0.049			
	Buffer[f] (298)	574	0.23	0.0021			
	Glass[g] (77)	506	6.06				
2	CH_2Cl_2 (298)	552	1.03	0.12	1.00 (0.19)	7.86 (0.30)	1.00 (0.19)
	CH_3CN (298)	568	0.47	0.038			
	Buffer[f] (298)	572	0.31	0.0030			
	Glass[g] (77)	502	5.57				
3	CH_2Cl_2 (298)	550	0.86	0.22	1.00 (0.20)	3.05 (0.25)	1.09 (0.19)
	CH_3CN (298)	573	0.32	0.037			
	Buffer[f] (298)	577	0.24	0.0023			
	Glass[g] (77)	505	5.90				
4	CH_2Cl_2 (298)	552	1.05	0.20	1.00 (0.21)	1.00 (0.21)	1.09 (0.21)
	CH_3CN (298)	573	0.37	0.065			
	Buffer[f] (298)	571	0.25	0.0049			
	Glass[g] (77)	504	5.72				
1a	CH_2Cl_2 (298)	548	1.12	0.28	1.00 (0.11)	1.75 (0.21)	0.99 (0.11)
	CH_3CN (298)	568	0.40	0.086			
	Buffer[f] (298)	572	0.11	0.034			
	Glass[g] (77)	506	6.67				
2a	CH_2Cl_2 (298)	544	1.24	0.15	1.00 (0.18)	1.20 (0.26)	1.03 (0.19)
	CH_3CN (298)	562	0.52	0.065			
	Buffer[f] (298)	566	0.21	0.033			
	Glass[g] (77)	504	6.18				
3a	CH_2Cl_2 (298)	548	1.10	0.24	1.00 (0.12)	1.15 (0.16)	0.98 (0.12)
	CH_3CN (298)	568	0.40	0.054			
	Buffer[f] (298)	572	0.13	0.032			
	Glass[g] (77)	504	6.45				
4a	CH_2Cl_2 (298)	549	1.00	0.34	1.00 (0.13)	1.05 (0.13)	1.01 (0.13)
	CH_3CN (298)	565	0.45	0.057			
	Buffer[f] (298)	574	0.12	0.034			
	Glass[g] (77)	506	6.53				

Reproduced from Refs. [77,82], with permission of The American Chemical Society.

[a] In degassed solvents. Excitation wavelength = 455 nm except for lifetime measurements for which the excitation wavelength = 355 nm.

[b] Relative emission intensities in aerated 50 mM potassium phosphate buffer pH 7.4. [**1**] = 17.5 μM, [**2**] = 16.7 μM, [**3**] = 15.5 μM, [**4**] and [**1a**]–[**4a**] = 15.2 μM.

[c] [avidin] = 0 μM, [unmodified biotin] = 0 μM.

[d] [avidin] = 3.8 μM, [unmodified biotin] = 0 μM.

[e] [avidin] = 3.8 μM, [unmodified biotin] = 380.0 μM.

[f] In 50 mM potassium phosphate buffer pH 7.4 containing 2.5% DMSO.

[g] EtOH/MeOH (4:1, v/v).

higher solvent polarity and hydrogen bond interactions between the amide group of the dpqa ligand and water [81].

Binding of complexes **1**–**3** to avidin has been justified by the HABA assay [43]. The binding of HABA to avidin is associated with an absorption feature at ca. 500 nm. Since the affinity of HABA to avidin ($K_d = 6 \times 10^{-6}$ M) is much weaker than that of biotin (K_d = ca. 10^{-15} M) [50,51], addition of biotin will replace the bound HABA molecules from the protein, leading to a decrease in the absorbance at 500 nm. Addition of the rhenium(I) biotin complexes to a mixture of HABA and avidin decreases the absorbance at 500 nm, indicating that the bound HABA molecules are replaced by the rhenium(I) biotin complexes. The plots of $-\Delta A_{500\,nm}$ versus [Re]:[avidin] for complexes **1**–**3** show that the equivalence points occur at [Re]:[avidin] = from ca. 4.3 to 4.7. Assuming that avidin can only specifically bind the complexes at the four biotin-binding sites, the occurrence of equivalence points at [Re]:[avidin] > 4 reveals that the binding of these rhenium(I) biotin complexes to avidin is not substantially stronger than that of HABA. Similar to other luminescent rhenium(I) biotin complexes [76,77], complexes **1**–**3** display enhanced emission in the presence of avidin. At the equivalence points of emission titrations, complexes **1**–**3** reveal a ca. 3.1–8.1-fold increase in emission intensities and a ca. 1.3–1.8-fold extension in emission lifetimes (Table 1). The emission enhancement factors are related to the chain lengths of the spacer-arms between the luminophore and biotin moieties. Complex **1** shows an 8.1-fold increment whilst complex **3** displays a smaller enhancement factor of 3.1 (Table 1). It is likely that the C-6 aminocaproic acid spacer-arm of complex **3** renders the luminophore to be more exposed to the polar bulk solution even

after the biotin moiety binds to the protein. Also, the increase of rigidity for this complex is lower as a result of its longer and more flexible spacer-arm. Most importantly, the emission enhancement factors of complexes **1–3** (ca. 3.1–8.1) are significantly larger than those of the dpq biotin complexes **1a–3a** (ca. 1.2–1.8) (Table 1). These observations are the consequence of the very low emission intensities of the free rhenium(I) dpqa biotin complexes in aqueous solution (Table 1). The K_d values of the rhenium-avidin adducts range from ca. 1.6×10^{-9} to 6.7×10^{-8} M.

Anthracene has been employed to study the avidin-binding behaviour of the rhenium(I) biotin complexes. When anthracene is in close proximity to a luminescent rhenium(I) polypyridine complex, it quenches the emission of the complex via the exchange mechanism; meanwhile, its own fluorescence is also quenched by the rhenium(I) complex by RET [85]. Schanze and co-workers have exploited these quenching properties and designed a series of interesting rhenium(I)-spacer-anthracene complexes as probes for double-stranded DNA molecules [86,87]. In our studies, avidin is labeled with 9-anthraldehyde by reductive animation to yield a fluorescent conjugate An-Av. Monomeric avidin has nine lysine residues and the crystal structure of this protein shows that most of these resides are located at the surface and thus can be readily modified [52–54]. From the spectroscopic data, the [anthracene]:[avidin] ratio of the conjugate An-Av is determined to be ca. 4.4. In aqueous buffer, An-Av exhibits vibronically structured emission bands at ca. 420, 440 and 477(sh) nm, typical of the fluorescence of anthracene. Complexes **1–3** still display small emission enhancement at ca. 565 nm upon binding to the quencher-modified conjugate An-Av. The emission lifetimes of these complexes are increased from ca. 0.19 to 0.28 μs, attributable to the binding of the complexes to An-Av. However, this increase is less substantial compared to the titrations of native avidin with the complexes (Table 1), indicative of emission quenching of the complexes by the anthracene molecules. The fluorescence of An-Av is also quenched by the rhenium(I) biotin complexes. The emission spectra of anthracene-modified avidin in the absence and presence of complex **1** are shown in Fig. 2. The results of the titrations of An-Av with the same complex in the absence and presence of excess biotin are displayed in Fig. 3. At the equivalence points, complexes **1**, **2** and **3** reduce the fluorescence intensities of An-Av at 420 nm by ca. 60, 53 and 55%, respectively. However, An-Av also exhibits fluorescence quenching in the control experiments in which (i) the An-Av is blocked with excess biotin molecules (Fig. 3) and (ii) the biotin-free complex **4** is used as the titrant. The reasons are that (i) the added rhenium(I) complexes also absorb at the excitation wavelength and (ii) non-specific hydrophobic interactions exist between the complexes and conjugate. However, in these controls, no equivalence points are observed and the fluorescence is lowered by only ca. 14% at [Re]:[An-Av] = 4:1. The higher extents of quenching of An-Av by complexes **1–3** indicate that the quenching is a consequence of the specific binding of the complexes to An-Av. The fluorescence quenching of anthracene possibly occurs via the distance-dependent RET mechanism [86,87]. This is reasonable because docking studies of a related ruthenium(II) biotin

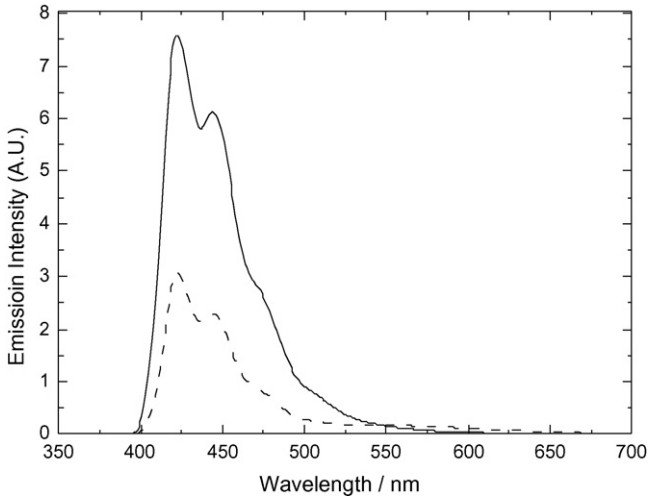

Fig. 2. Emission spectra of An-Av (3.8 μM) in the presence of 0 (—) and 17.3 (- - -) μM of complex **1** in 50 mM potassium phosphate buffer pH 7.4/DMSO (97:3, v/v) at 298 K. Reproduced from Ref. [82], with permission of The American Chemical Society.

complex reveal that while the biotin moiety is bound at the substrate pocket of the protein, the metal polypyridine unit is actually located on the surface [67]. Thus, it is conceivable that our rhenium(I) polypyridine moieties can interact with the surface anthracene molecules, resulting in emission quenching by RET. The K_d value for the binding of complex **1** to the conjugate An-Av is determined to be ca. 4.1×10^{-7} M.

The interesting emission properties of iridium(III) polypyridine complexes [88–94] and our recent interest in using these complexes as biological labelling reagents [21,38,40,42] have prompted us to design new iridium(III) biotin complexes. Luminescent cyclometallated iridium(III) complexes containing an extended planar diimine ligand, $[Ir(ppy)_2(N{-}N)](PF_6)$ (N–N = dpq (**5**), dpqa (**6**), dpqB (**7**), dppz (**8**), dppn (**9**), dppzB (**10**)) (Fig. 4) have been studied [95]. Upon photoexcitation, complexes **5–10** display long-lived green to orange luminescence (Table 2). The emission of complexes **5–9** in fluid solutions is assigned to a ^{3}MLCT ($d\pi(Ir) \rightarrow \pi^*(N{-}N)$) excited

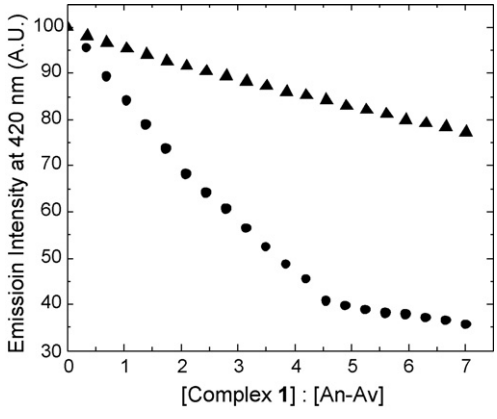

Fig. 3. Luminescence titration curves for the titrations of (i) 3.8 μM An-Av (●), and (ii) 3.8 μM An-Av and 380 μM unmodified biotin (▲) with complex **1**. The emission intensities of the solution at 420 nm are monitored. Reproduced from Ref. [82], with permission of The American Chemical Society.

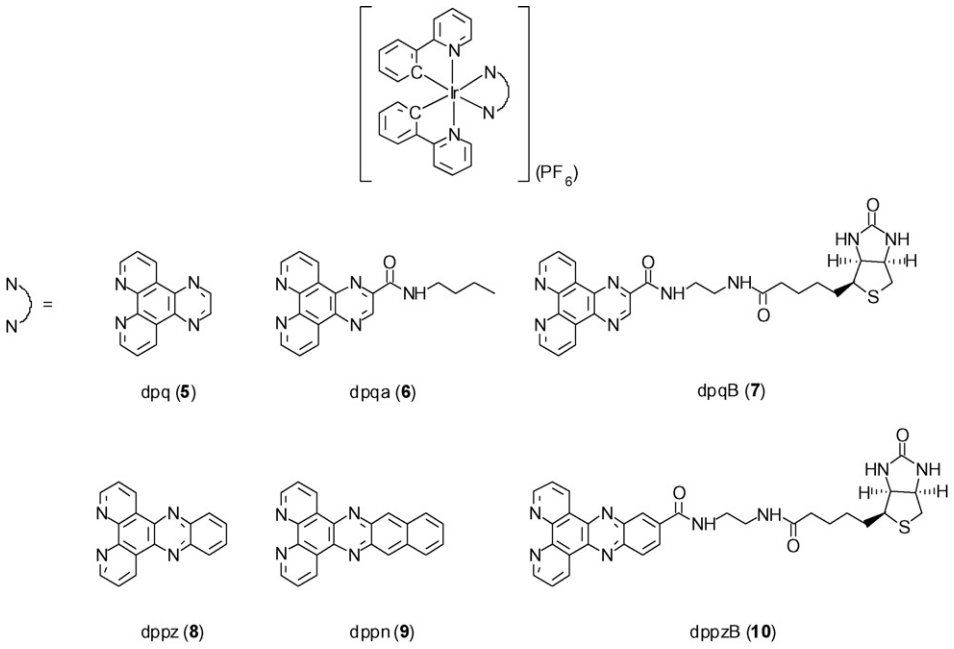

Fig. 4. Structures of complexes **5**–**10**. Reproduced from Ref. [95], with permission of Wiley–VCH.

Table 2
Photophysical data of complexes **5**–**10**

Complex	Medium (T (K))	λ_{em} (nm[a])	τ_o (μs[a])	Φ_{em}[a]
5	CH_2Cl_2 (298)	590	0.67	0.24
	CH_3CN (298)	601	0.34	0.11
	MeOH (298)	603	0.18	0.064
	Glass[b] (77)	528, 561 sh	4.72	
6	CH_2Cl_2 (298)	599	0.48	0.17
	CH_3CN (298)	608	0.13	0.034
	MeOH (298)	598	1.46 (8%), 0.14 (92%)	0.0009
	Glass[b] (77)	532, 566 sh	3.86	
7	CH_2Cl_2 (298)	597	0.43	0.13
	CH_3CN (298)	606	0.09	0.019
	MeOH (298)	596	1.13 (7%), 0.15 (93%)	0.0006
	Glass[b] (77)	529, 565 sh	3.93	
8	CH_2Cl_2 (298)	603	0.56	0.072
	CH_3CN (298)	630	0.077	0.0023
	MeOH (298)	600	0.38	$<10^{-4}$
	Glass[b] (77)	544 (max), 563 sh, 589, 643 sh	1224	
9	CH_2Cl_2 (298)	585	0.58	0.0016
	CH_3CN (298)	588	0.36	0.0012
	MeOH (298)	583	0.42	0.0016
	Glass[b] (77)	535	4.45	
10	CH_2Cl_2 (298)	510, 535 sh	0.71	0.019
		654 sh	0.13	
	CH_3CN (298)	492 sh,520	1.40	0.0064
		612 sh	0.83	
	MeOH (298)	490, 530, 556 (max)	1.71	0.0010
		650 sh	0.36	
	Glass[b] (77)	547 (max), 591, 644 sh	1040	

Reproduced from Ref. [95], with permission of Wiley–VCH.
[a] In degassed solvents. Excitation wavelength = 455 nm except for lifetime measurements for which the excitation wavelength = 355 nm.
[b] EtOH/MeOH (4:1, v/v).

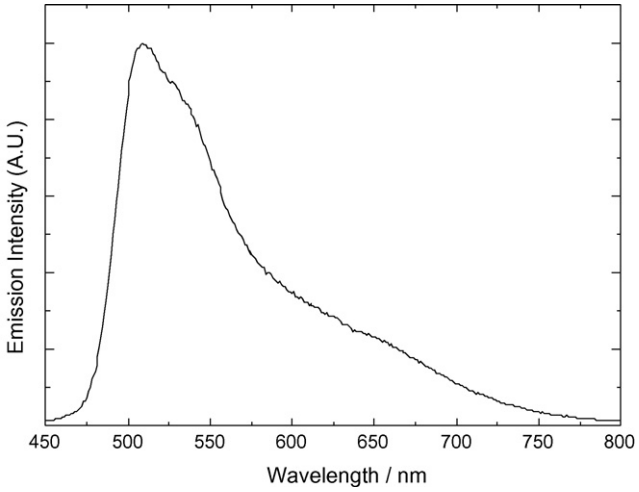

Fig. 5. Emission spectrum of complex **10** in CH_2Cl_2 at 298 K. Reproduced from Ref. [95], with permission of Wiley–VCH.

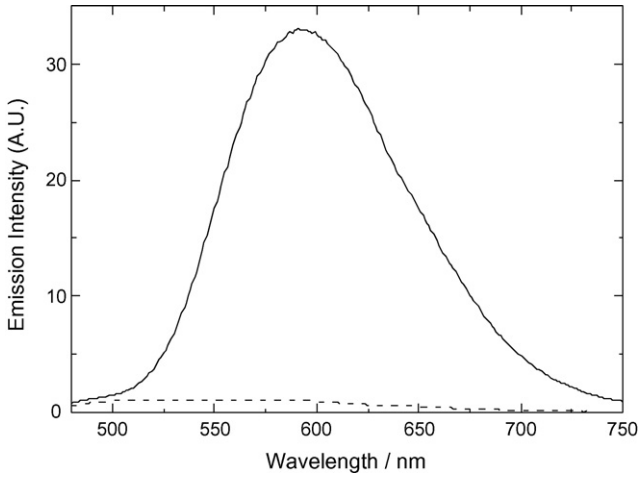

Fig. 6. Emission spectra of complex **5** (137 μM) in a mixture of Tris-Cl buffer (50 mM, pH 7.4) and methanol (7:3, v/v) in the absence (- - -) and presence (—) of double-stranded calf thymus DNA (744 μM). Reproduced from Ref. [95], with permission of Wiley–VCH.

state, which is supported by the shorter emission lifetimes and lower emission quantum yields of the complexes in more polar solvents such as CH_3CN and MeOH than in less polar CH_2Cl_2 (Table 2). Among complexes **5**–**7**, the decrease of the emission quantum yields on going from CH_2Cl_2 to MeOH is much more significant for the amido complexes **6** and **7** compared to the dpq complex **5** (Table 2). Similar to the rhenium(I) dpqa system described above, the reduced quantum yields of complexes **6** and **7** are due to hydrogen bonding interactions between the amide groups of the diimine ligands and protic solvent molecules [81]. Among the dppz and dppn complexes **8**–**10**, complexes **8** and **10** also show solvent-dependent emission quantum yields (Table 2). Both complexes do not emit in aqueous solution; hydrogen bonding interactions between the phenazine nitrogens of both complexes (and the amide moiety of complex **10**) and water molecules may also exist [96,97]. The dppn complex **9** does not display similar solvent-dependent emission but exhibits very similar emission lifetimes and quantum yields in different solvents, suggestive of a ^{3}IL ($\pi \rightarrow \pi^*$) (dppn) emissive state. Unlike complexes **5**–**9**, the dppzB complex **10** displays dual emission in fluid solutions at room temperature; for example, the emission spectrum of this complex in CH_2Cl_2 displays two emission features (Fig. 5). The higher-energy emission band at ca. 510 nm is tentatively assigned to an excited state of ^{3}IL ($\pi \rightarrow \pi^*$) (dppzB) character in view of its longer emission lifetime ($\tau_o = 0.71$ μs) and structural features. The lower-energy emission shoulder at ca. 654 nm is of a shorter lifetime ($\tau_o = 0.13$ μs), which is likely to originate from a ^{3}MLCT ($d\pi(Ir) \rightarrow \pi^*$ (dppzB)) excited state.

Of the six complexes, the biotin-free complexes **5**, **6**, **8** and **9** display emission enhancement in the presence of double-stranded calf thymus DNA. The emission intensity of the dpq complex **5** at ca. 591 nm is enhanced by ca. 33-fold (Fig. 6). Both the dpqa complex **6** and the dppz complex **8** do not emit in aqueous buffer solution. However, upon addition of double-stranded DNA, new emission bands are observed at ca. 602 and 606 nm for these two complexes, respectively; the emission intensities are ca. 40 and 12 times that of the background in the absence of DNA. The emission enhancement is ascribed to the intercalation of the complexes to the base-pairs of the double-stranded DNA molecules [96,97]. Although the photophysical properties of the biotin complexes **7** and **10** are very similar to those of their dpq and dppz counterparts (complexes **5** and **8**), respectively, their spectra do not show any changes in the DNA titration experiments. It is likely that the steric bulk of the biotin moiety inhibits the complexes from intercalating into the double-stranded DNA molecules.

The avidin-binding properties of complexes **7** and **10** have been confirmed by HABA assays [43]. Although both complexes are non-emissive in aqueous buffer, addition of avidin leads to the appearance of a new emission band with a maximum at ca. 490 nm and a shoulder at ca. 520 nm. The emission spectra of complex **7** in the absence and presence of avidin are displayed in Fig. 7. At [Ir]:[avidin] = 4, the emission intensities of complexes **7** and **10** at 490 nm are increased by ca. 31- and 8-fold, respec-

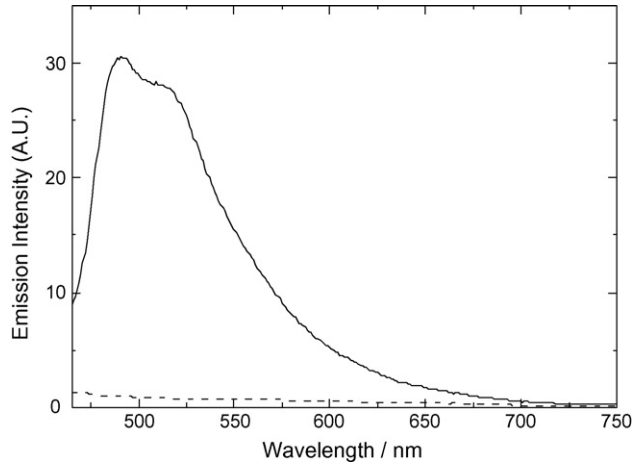

Fig. 7. Emission spectra of complex **7** (22 μM) in a mixture of potassium phosphate buffer (50 mM, pH 7.4) and methanol (9:1, v/v) in the absence (- - -) and presence (—) of avidin (5.5 μM). Reproduced from Ref. [95], with permission of Wiley–VCH.

tively. Interestingly, the emission band of the adduct $(\mathbf{7})_4$-avidin occurs at much higher energy compared to the free complex in organic solvents (ca. 596–606 nm) (Table 2) and the DNA-adducts of the dpq complex **5** and dpqa complex **6** (ca. 591 and 602 nm, respectively). The appearance of a new emission band for this iridium(III) biotin complex at higher energy could be partly due to the hydrophobic biotin-binding site of the protein because many cyclometallated iridium(III) polypyridine complexes possess solvatochromic behaviour [88–94]. However, complex **7** does not show very different emission wavelengths in different solvents (Table 2), and such a large difference in emission energy (ca. 3755 cm^{-1}) compared to the DNA adduct of the dpqa complex **6** cannot be solely due to hydrophobic effects. The most probable reason is that the emission of this adduct originates from a state of higher energy than the MLCT state, which is likely to be a state of predominant ^{3}IL ($\pi \rightarrow \pi^*$) (dpqB) character. This assignment is supported by the long emission lifetime (ca. 2.2 μs) and the vibronic features of the emission band. The reason for the switching of excited-state nature from supposedly ^{3}MLCT ($d\pi(Ir) \rightarrow \pi^*$(dppzB)) to ^{3}IL ($\pi \rightarrow \pi^*$) (dppzB) is unknown at this stage. However, these observations could be unique to cyclometallated iridium(III) polypyridine complexes because the ^{3}IL/^{3}MLCT emission of these complexes responds very sensitively to subtle changes of the identity of the cyclometallating and polypyridine ligands as well as their local environments [88–94]. Emission titration studies show that the adduct $(\mathbf{6})_4$-avidin also displays a structured emission band at ca. 490 nm (a spacing of ca. 1177 cm^{-1}) with a lifetime of 1.8 μs. This band is tentatively assigned to an excited state of ^{3}IL ($\pi \rightarrow \pi^*$) (dppzB) character. The K_d values of complexes **7** and **10** are determined to be 2.0×10^{-7} and 8.2×10^{-7} M, respectively.

A new series of luminescent ruthenium(II) dpq-biotin complexes $[Ru(N\text{–}N)_2(N\text{–}N')](PF_6)_2$ (N–N = bpy, N–N′ = dpqB (**11a**), dpq-C6-B (**11b**); N–N = phen, N–N′ = dpqB (**12a**), dpq-C6-B (**12b**); N–N = Ph_2-phen, N–N′ = dpqB (**13a**), dpq-C6-B (**13b**)) (Fig. 8) has been synthesised and characterised [98]. All the complexes feature intense ^{1}IL ($\pi \rightarrow \pi^*$) (N–N) absorption bands at ca. 258–286 nm (ε on the order of 10^4 dm^3 mol^{-1} cm^{-1}) and ^{1}MLCT ($d\pi(Ru) \rightarrow \pi^*$(N–N)) bands in the visible region (ca. 420–458 nm). Interestingly, all these complexes do not show a remarkably low-energy ^{1}MLCT absorption band associated with the dpq-biotin ligands despite their extended π-conjugation, suggestive of the bichromophoric (i.e. "bpy" and "quinoxaline-amide") character of these ligands [99]. The ruthenium(II) dpq-biotin complexes exhibit orange-red ^{3}MLCT ($d\pi(Ru) \rightarrow \pi^*$(N–N)) emission upon visible-light excitation (Table 3). While the emission energies of the complexes are very similar, the Ph_2-phen complexes **13a** and **13b** display more intense and longer-lived emission than the other complexes (Table 3). In addition, the photophysical properties of the complexes are comparable to those of their corresponding homoleptic counterparts $[Ru(bpy)_3]^{2+}$ [100,101], $[Ru(phen)_3]^{2+}$ [102] and $[Ru(Ph_2\text{-phen})_3]^{2+}$ [103] in CH_3CN. These results suggest the possible involvement of the ancillary diimine ligands in the ^{3}MLCT emissive states of the current complexes. Similar to the rhenium(I) and iridium(III) dpqa and/or dpqB

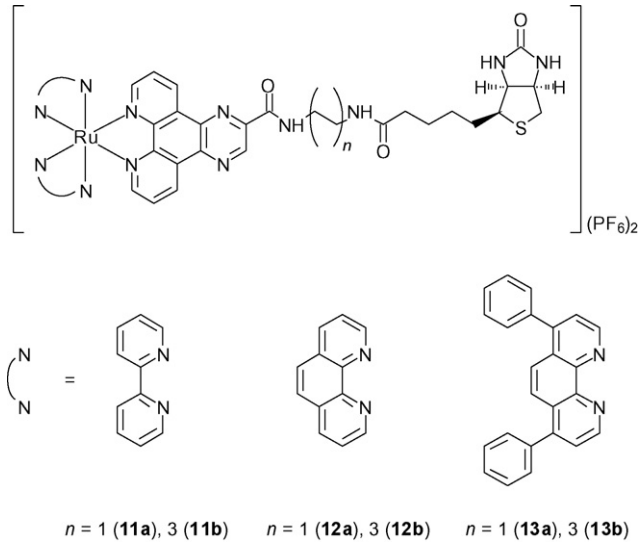

Fig. 8. Structures of complexes **11a**–**13a**, and **11b**–**13b**. Reproduced from Ref. [98], with permission of Elsevier.

complexes described above, the emission quantum yields of the ruthenium(II) complexes decrease substantially from CH_3CN to aqueous buffer (Table 3). These quantum yield values are much lower than that of the related complex $[Ru(bpy)_2(dpq)]^{2+}$ in buffer, highlighting the interactions between the amide moiety of the dpq-biotin ligand and water molecules [81]. Interestingly, Meyer and co-workers reported that the solvent-induced light-switch behaviour of $[Ru(bpy)_2(dppz)]^{2+}$ originates from a dynamic equilibrium between a "dark" and a "bright" MLCT state [104,105]. The "dark" MLCT state localises on the phenazine fragment of dppz ligand, which is lower in energy than the bpy-based "bright" MLCT state. A similar model could account for the different emission properties of the ruthenium(II) dpq-biotin complexes in CH_3CN and buffer. Although it is possible that the LUMO's of the complexes involve the quinoxaline moiety of the dpq-biotin ligands as concluded in related systems [99], the bpy-fragment of these dpq-biotin ligands or the ancillary diimine ligands (especially the Ph_2-phen ligands in the cases of complexes **13a** and **13b** due to their long lifetimes) may contribute to the "bright" MLCT emission in CH_3CN. In aqueous solution, it is probable that the "dark" state associated with the quinoxaline-fragment of the dpq-biotin ligands is stabilised by hydrogen-bonding interactions between their amide moieties and water molecules, resulting in very low emission quantum yields of the complexes [81].

Addition of avidin to the current ruthenium(II) dpq-biotin complexes in aqueous buffer results in emission enhancement. As an example, the emission spectra of complex **13b** in the absence and presence of avidin in aqueous buffer are shown in Fig. 9. At [avidin]:[Ru] = 0.25, the emission intensities of the complexes are increased by ca. 3.8–8.2-fold (Table 3 and Fig. 10 for complex **13b**). The excited-state lifetimes of the complexes are also elongated from 0.3–0.6 to 0.6–1.3 μs (Table 3). The degree of emission intensity enhancement depends strongly on the diimine ligands and follows the order: Ph_2-phen > phen > bpy, which is in accordance with our previ-

Table 3
Photophysical data of complexes **11a–13a** and **11b–13b**

Complex	Medium (T (K))	λ_{em} (nm[a])	τ_o (μs[a])	Φ_{em}[a]	I (τ (ns))[b,c]	I (τ (ns))[b,d]	I (τ (ns))[b,e]
11a	CH_3CN (298)	616	1.05	0.058	1.00 (263)	4.57 (561)	1.14 (270)
	Buffer[f] (298)	620	0.79	0.0009			
	Glass[g] (77)	582 (max), 629, 683 sh	5.83				
11b	CH_3CN (298)	616	1.12	0.057	1.00 (298)	3.83 (848)	1.11 (324)
	Buffer[f] (298)	619	0.73	0.0010			
	Glass[g] (77)	583 (max), 626, 686 sh	5.98				
12a	CH_3CN (298)	612	0.85	0.067	1.00 (290)	5.26 (1017)	1.09 (286)
	Buffer[f] (298)	617	0.83	0.0006			
	Glass[g] (77)	574 (max), 618, 677 sh	7.65				
12b	CH_3CN (298)	611	1.09	0.073	1.00 (355)	5.89 (999)	1.05 (342)
	Buffer[f] (298)	615	0.89	0.0010			
	Glass[g] (77)	570 (max), 615, 677 sh	7.73				
13a	CH_3CN (298)	613	2.56	0.12	1.00 (606)	5.94 (1149)	1.13 (607)
	Buffer[f] (298)	617	1.55	0.0009			
	Glass[g] (77)	589 (max), 634, 690 sh	7.98				
13b	CH_3CN (298)	613	2.57	0.11	1.00 (464)	8.24 (1264)	1.51 (484)
	Buffer[f] (298)	617	1.62	0.0013			
	Glass[g] (77)	590 (max), 641, 692 sh	8.38				

Reproduced from Ref. [98], with permission of Elsevier.
[a] In degassed solvents. Excitation wavelengih = 455 nm except for lifetime measurements for which the excitation wavelength = 355 nm.
[b] Relative emission intensities in aerated 50 mM potassium phosphate buffer pH 7.4. [Ru] = 2.8 μM.
[c] [avidin] = 0 μM, [unmodified biotin] = 0 μM.
[d] [avidin] = 0.70 μM, [unmodified biotin] = 0 μM.
[e] [avidin] = 0.70 μM, [unmodified biotin] = 70 μM.
[f] In 50 mM potassium phosphate buffer pH 7.4 containing 10% DMSO.
[g] EtOH/MeOH (4:1, v/v).

ous observations that more hydrophobic transition metal biotin complexes exhibit more significant avidin-induced emission amplification [76–79]. Most importantly, the avidin-induced emission enhancement factors of the current ruthenium(II) dpq-biotin complexes (ca. 3.8–8.2) are much larger than those of related ruthenium(II) bipyridine [80] and phenanthroline [68] biotin complexes (1.2–1.6-fold). The reason is that the free ruthenium(II) dpq-biotin complexes show extremely weak emission in aqueous buffer. The K_d values vary from ca. 6.2×10^{-9} to 9.5×10^{-8} M. The current ruthenium(II) dpq-biotin complexes show significant broad ^{1}MLCT absorption bands at ca. 450 nm, which is similar in energy to the 488-nm excitation of an argon laser, rendering them promising candidates as probes for immunoassays and in vitro analysis using laser-scanning confo-

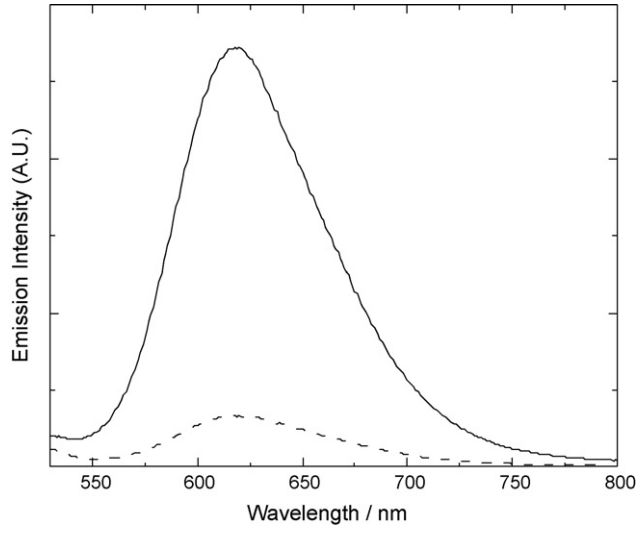

Fig. 9. Emission spectra of complex **13b** (2.8 μM) in the absence (- - -) and presence of 0.70 μM (—) of avidin in potassium phosphate buffer at 298 K. Reproduced from Ref. [98], with permission of Elsevier.

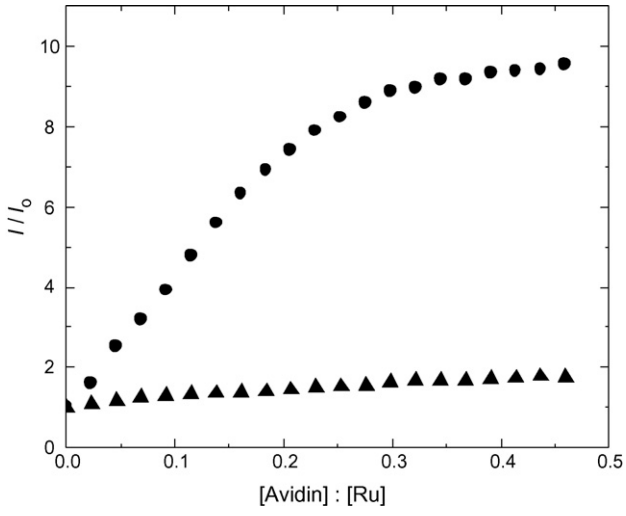

Fig. 10. Luminescence titration curves for the titrations of complex **13b** (2.8 μM) with avidin (●) and biotin-blocked avidin (▲). Reproduced from Ref. [98], with permission of Elsevier.

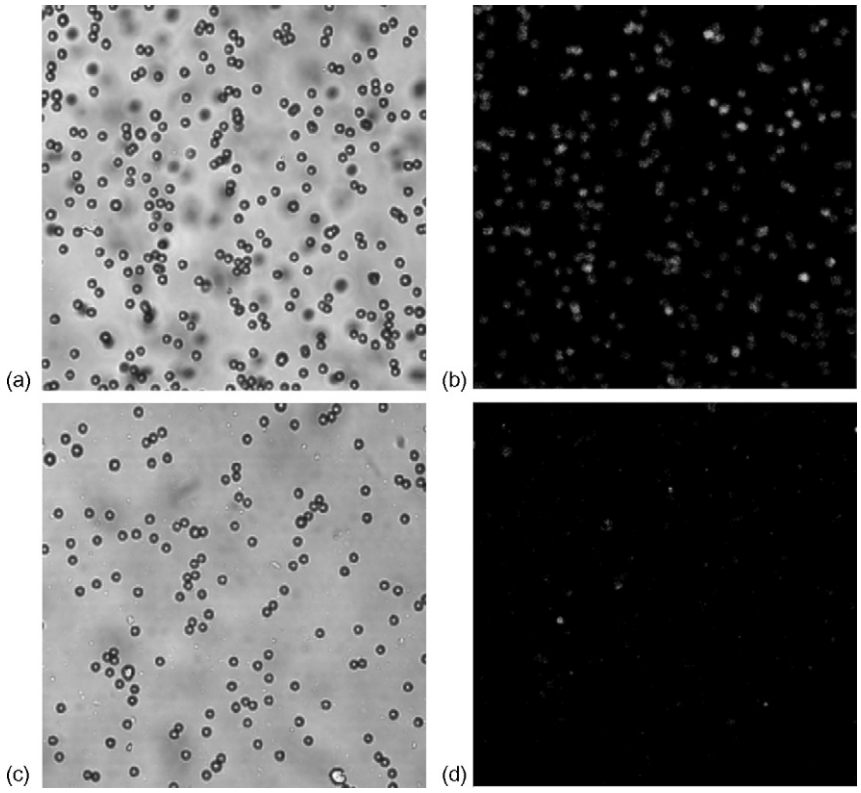

Fig. 11. Bright field (a) and fluorescent (b) images of a buffer solution containing avidin-modified microspheres and complex **11a** in the absence of biotin. (c and d): Conditions are the same as those of (a) and (b), respectively, except that the avidin molecules used are blocked by excess biotin. Reproduced from Ref. [98], with permission of Elsevier.

cal microscopy. To investigate these possibilities, the binding of complex **11a** to avidin molecules immobilised on microsphere particles has been examined. A solution of complex **11a** is added to avidin-coated microspheres in the absence and presence of excess biotin, respectively, and the samples are visualised with a confocal microscope. Bright field and fluorescent images of these two sample solutions are shown in Fig. 11(a–d). Without excess biotin, the avidin-modified microspheres reveal intense luminescence upon excitation owing to avidin-bound complex **11a** on the surface of the particles (Fig. 11(b)). However, when excess biotin is initially present, addition of complex **11a** to the microspheres only results in a very small number of weakly luminescent particles (Fig. 11(d)), indicating the lack of substantial binding of the complex to the immobilised protein. These results demonstrate that the current ruthenium(II) dpq-biotin complexes can act as luminescent probes for immobilised avidin and can be employed in the development of new heterogeneous bioassays.

3. Indole complexes

The indole unit occurs naturally in a variety of structures and over a thousand indole alkaloids are known to date. Due to the broad existence and the important physiological activities of these indole compounds [106,107], the search for their specific receptors has been met with increasing attention. Serum albumins are the most common indole-binding proteins in the circulatory system and are responsible for the maintenance of blood pH and colloid osmotic blood pressure [108]. The unique capability of albumins is their reversible binding of a large number of endogenous and exogenous compounds. Serum albumins contain six specific binding sites including two for small heterocyclic or aromatic carboxylic acids (sites I and II), two for long-chain fatty acids (sites III and IV) and two for metal ions (sites V and VI) [109–111]. Indole and its derivatives are believed to bind to site II of serum albumins [109–111]. Tryptophanase (TPase) is another indole-binding protein that catalyses the α,β-elimination and β-replacement reactions of various substrates such as L-tryptophan in the presence of the cofactor pyridoxal 5-phosphate [112,113]. Indole has been found to inhibit the catalytic functions of this protein [112,113].

The design of biological probes for indole-binding proteins relies mainly on functionalised indole derivatives. Various approaches such as radioactive and fluorescent labels [114–116], enzyme inhibition assays [117,118] and biotinylated indole compounds [119] have been used. In fact, the fluorescence of indole and its derivatives is sensitive to the environment and thus these compounds have been exploited as reporters of their surroundings [116,120]. Although indole and its derivatives have been used as ligands to form a number of transition metal complexes [121], the incorporation of an indole unit into luminescent transition metal complexes to develop probes for indole-binding biomolecules has not been explored. In view of the remarkable luminescence properties of rhenium(I) polypyridine complexes [83,84], we have utilised the indole complexes $[Re(N{-}N)(CO)_3(L)](CF_3SO_3)$ (N–N = Me_4-phen, L = py-3-

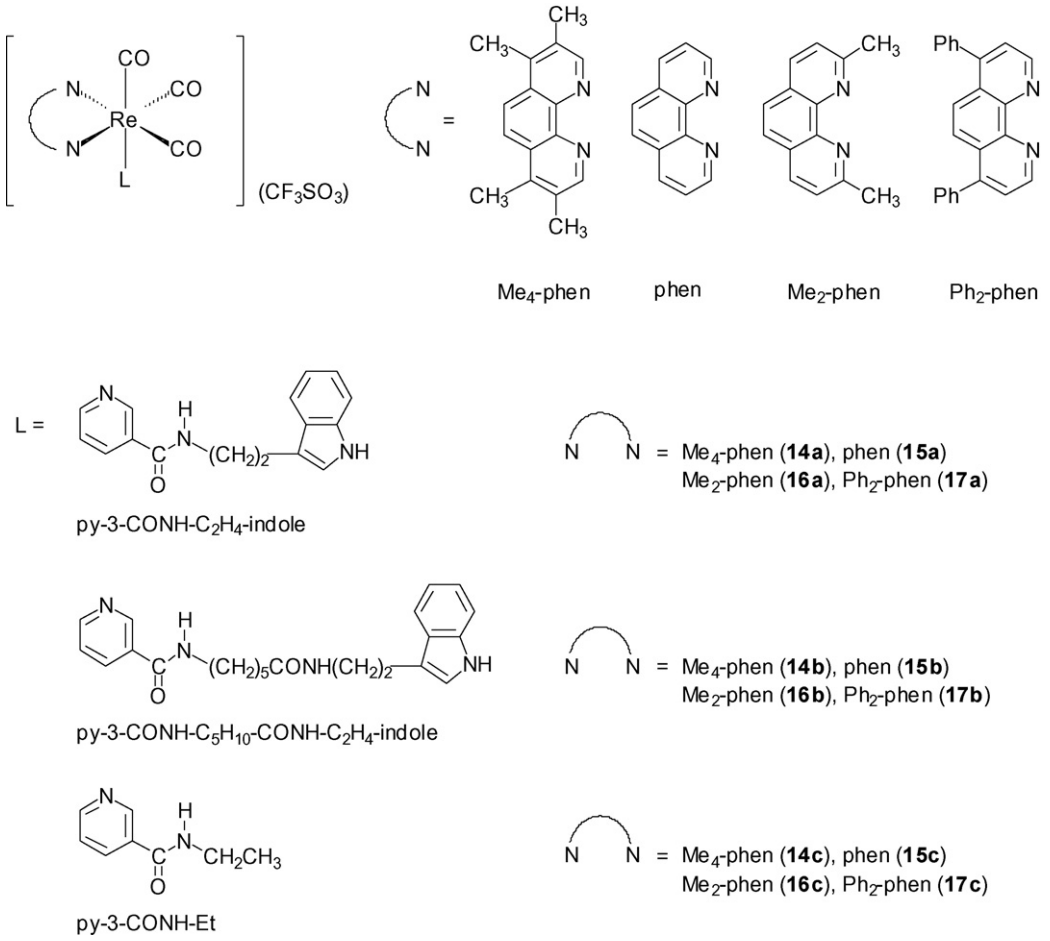

Fig. 12. Structures of complexes **14a**–**17a**, **14b**–**17b** and **14c**–**17c**. Reproduced from Ref. [123], with permission of The American Chemical Society.

CONH-C_2H_4-indole (**14a**), py-3-CONH-C_5H_{10}-CONH-C_2H_4-indole (**14b**); N–N = phen, L = py-3-CONH-C_2H_4-indole (**15a**), py-3-CONH-C_5H_{10}-CONH-C_2H_4-indole (**15b**); N–N = Me_2-phen, L = py-3-CONH-C_2H_4-indole (**16a**), py-3-CONH-C_5H_{10}-CONH-C_2H_4-indole (**16b**); N–N = Ph_2-phen, L = py-3-CONH-C_2H_4-indole (**17a**), py-3-CONH-C_5H_{10}-CONH-C_2H_4-indole (**17b**)) (Fig. 12) as probes for indole-binding proteins [122,123]. Their indole-free counterparts [Re(N–N)$(CO)_3$(py-3-CONH-Et)](CF_3SO_3) (N–N = Me_4-phen (**14c**), phen (**15c**), Me_2-phen (**16c**), Ph_2-phen (**17c**)) (Fig. 12) have also been studied.

Upon visible-light excitation, all the complexes display green to orange-yellow luminescence under ambient conditions (Table 4). The solution emission of these indole-containing complexes is generally assigned to a ^{3}MLCT ($d\pi(Re) \rightarrow \pi^*$(N–N)) excited state [83,84]. However, the structural features and long emission lifetimes of the Me_4-phen complexes **14a**–**14c** in solutions at room temperature (Table 4) suggest that the excited state of these complexes exhibits substantial ^{3}IL ($\pi \rightarrow \pi^*$) (Me_4-phen) character. When the indole-containing complexes are excited in the ultra-violet region (λ_{ex} = 250 nm), they exhibit an additional emission band at ca. 365 nm that originates from the indole moiety.

The rhenium(I) indole complexes display much lower luminescence quantum yields and shorter emission lifetimes than those of their indole-free counterparts (Table 4). Also, unlike their indole-free counterparts, these complexes show concentration-dependent emission lifetimes, suggesting a self-quenching process. The self-quenching rate constants (k_{sq}) and lifetimes at infinite dilution ($\tau_{i.d.}$) of the indole-containing complexes in CH_3CN have been determined from plots of τ^{-1} versus [Re] to be on the order of 10^9 dm^3 mol^{-1} s^{-1} and 2.1–13.9 μs, respectively. These emission lifetimes are comparable to those of the indole-free complexes **14c**–**17c** (Table 4), indicative of the importance of intermolecular interactions in the self-quenching of the complexes. As the triplet-state energy of indole (ca. 24,800 cm^{-1}) [124] is much higher than the emission energy of the rhenium(I) indole complexes, and there is no spectral overlap between the emission band of the indole-free complexes and the absorption band of indole, it is unlikely that the self-quenching of the indole-containing complexes occurs via an energy-transfer mechanism. From the potentials of the diimine-based reduction of [Re(N–N)$(CO)_3$(py-3-CONH-Et)]$^+$ (between ca. −1.1 and −1.4 V versus SCE) and the low-temperature emission energy of [Re(N–N)$(CO)_3$(py-3-CONH-Et)]$^+$ (E^{00} = 2.44–2.67 eV), the excited-state reduction potentials, E^0[$Re^{+*/0}$], are estimated to be ca. +1.25 to +1.49 V versus SCE. On the basis of these potentials and the redox potential of indole (E^0[indole$^{+/0}$] < +1.06 V versus SCE), reductive quenching of the excited complexes by indole is favoured by >0.2–0.4 eV. It is likely that the mechanism

Table 4
Photophysical data and results of BSA-titrations and TPase-inhibition assays for complexes **14a–17a**, **14b–17b** and **14c–17c**

Complex	Medium (T (K))	λ_{em} (nm[a])	τ_o (μs[a])	Φ_{em}[a]	I/I_o[b,c]	τ/τ_o[b,d]	K_a (M^{-1}[b,e])	n[b,f]	Inhibition (%[g,h])	K_m (mM[g,i])
14a	CH_3CN (298)	518	8.21	0.0085	2.4	1.7	1.0×10^4	0.6	61	143
	MeOH (298)	516	8.60	0.0083						
	Buffer[j] (298)	516	8.14	0.0057						
	Glass[k] (77)	464, 497, 530 sh	86.38 (52%), 19.77 (48%)							
14b	CH_3CN (298)	514	6.33	0.0091	17.1	2.0	1.7×10^4	0.7	74	172
	MeOH (298)	520	6.19	0.0035						
	Buffer[j] (298)	514	6.11	0.0053						
	Glass[k] (77)	465, 497, 533, 540 sh	95.17 (49%), 21.43 (51%)							
14c	CH_3CN (298)	515	14.12	0.54	1.1	1.0	–[l]	–[l]	3	166
	MeOH (298)	516	14.25	0.39						
	Buffer[j] (298)	515	12.83	0.25						
	Glass[k] (77)	464, 497, 534 sh, 577 sh	117.65 (44%), 28.98 (56%)							
15a	CH_3CN (298)	548	1.91	0.021	2.1	1.3	0.9×10^4	0.5	43	154
	MeOH (298)	548	1.36	0.019						
	Buffer[j] (298)	550	1.06	0.014						
	Glass[k] (77)	476 sh, 494	10.11							
15b	CH_3CN (298)	545	1.87	0.020	3.2	1.3	1.1×10^4	0.8	72	179
	MeOH (298)	547	1.31	0.016						
	Buffer[j] (298)	548	1.09	0.0093						
	Glass[k] (77)	462 sh, 497	10.23							
15c	CH_3CN (298)	548	2.11	0.33	1.1	1.1	–[l]	–[l]	7	154
	MeOH (298)	546	1.56	0.23						
	Buffer[j] (298)	548	1.16	0.17						
	Glass[k] (77)	476 sh, 494	11.21							
16a	CH_3CN (298)	530	1.79	0.0076	8.1	1.6	0.9×10^4	0.5	64	161
	MeOH (298)	532	1.66	0.0059						
	Buffer[j] (298)	532	1.47	0.0049						
	Glass[k] (77)	475 sh, 496	15.31							
16b	CH_3CN (298)	534	1.62	0.038	5.0	1.3	1.1×10^4	0.7	74	167
	MeOH (298)	537	1.72	0.018						
	Buffer[j] (298)	536	1.55	0.0089						
	Glass[k] (77)	470 sh, 497	15.67							
16c	CH_3CN (298)	536	2.30	0.30	1.3	1.1	–[l]	–[l]	8	157
	MeOH (298)	531	2.57	0.30						
	Buffer[j] (298)	533	2.10	0.24						
	Glass[k] (77)	475 sh, 497	15.69							
17a	CH_3CN (298)	558	4.38	0.029	1.0	1.1	–[l]	–[l]	55	158
	MeOH (298)	556	3.96	0.021						
	Buffer[j] (298)	561	2.99	0.015						
	Glass[k] (77)	508, 534 sh	22.78							
17b	CH_3CN (298)	554	3.82	0.037	1.1	1.1	–[l]	–[l]	77	176
	MeOH (298)	556	3.62	0.036						
	Buffer[j] (298)	561	3.05	0.016						
	Glass[k] (77)	508, 534 sh	22.99							
17c	CH_3CN (298)	560	6.06	0.34	0.9	1.0	–[l]	–[l]	6	154
	MeOH (298)	556	5.04	0.27						
	Buffer[j] (298)	562	3.36	0.18						
	Glass[k] (77)	508, 534 sh	23.68							

Reproduced from Ref. [123], with permission of The American Chemical Society.
[a] In degassed solvents. Excitation wavelength = 355 nm. [Re] = 50 μM.
[b] In 50 mM potassium phosphate buffer pH 7.4 at 298 K.
[c] I_o and I are the emission intensities in the presence of 0 and 1 mM BSA, respectively.
[d] τ_o and τ are the emission lifetimes in the presence of 0 and 1 mM BSA, respectively.
[e] Binding constants to BSA.
[f] Binding stoichiometries to BSA.
[g] In 0.15 mM potassium phosphate buffer pH 8.0 at 310 K.
[h] Percentage inhibition of TPase activity by the rhenium(I) polypyridine complexes at [L-serine] = 800 mM.
[i] Michaelis constants for TPase assays.
[j] In 50 mM potassium phosphate buffer pH 7.4 containing 20% MeOH.
[k] EtOH/MeOH (4:1, v/v).
[l] These complexes do not show BSA-binding properties.

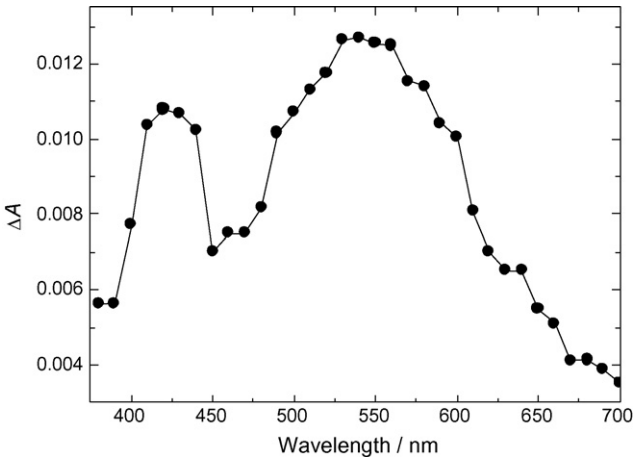

Fig. 13. Transient absorption difference spectrum of a degassed acetonitrile solution of complex **16c** (5.5 mM) and indole (55 mM) at 298 K recorded 6 μs after laser flash. Reproduced from Ref. [123], with permission of The American Chemical Society.

of the emission quenching of the rhenium(I) indole complexes is electron-transfer in nature. To obtain more direct spectroscopic information on the mechanism of the photo-reactions between the indole-free complexes **14c**–**17c** and indole, nanosecond transient absorption experiments have been performed. The transient absorption difference spectrum of an acetonitrile solution of complex **16c** and indole at 298 K recorded 6 μs after laser flash is shown in Fig. 13. The spectrum displays an absorption band at ca. 420 nm and a broader one of higher intensity at ca. 550 nm. It is unlikely that these bands are associated with diimine-localised anion of the rhenium(I) polypyridine complex, $[Re^{I}(Me_2\text{-}phen^{\bullet -})(CO)_3(py\text{-}3\text{-}CONH\text{-}Et)]^0$ because the absorption band of the diimine anion radical is expected to occur at ca. 350–400 nm [125,126]. With reference to the pulse radiolysis and transient absorption studies of a series of indole derivatives [127,128], these bands at ca. 420 and 550 nm are assigned to the absorption of the indolyl radical. These results conclude that the emission quenching of the complexes by indole is electron-transfer in nature.

The interactions of the rhenium(I) indole complexes with BSA, an indole-binding protein, have been studied by emission titrations. The emission intensities of the indole-containing complexes are enhanced in the presence of BSA. At [BSA] = 1 mM, the indole-containing complexes reveal up to a 17-fold increase in emission intensities and a 2-fold increase in emission lifetimes (Table 4). These observations are ascribed to the specific binding of the indole moiety of the complexes to the protein. Previous studies show that indole and its derivatives bind to a specific hydrophobic site of BSA [109–111]. The increase in the emission intensities and lifetimes of the indole-containing complexes should be closely related to the enhanced hydrophobicity and rigidity of their local surroundings upon binding to the protein. Another possible reason is that intermolecular electron transfer between the rhenium(I) indole complexes is inhibited upon the protein-binding event. Nevertheless, in the cases of the Ph_2-phen complexes **17a** and **17b**, the emission properties do not show significant changes, which may be due to the relatively bulky Ph_2-phen ligand that inhibits the protein-binding of these complexes. The binding constants (K_a) of the complexes to BSA and the binding stoichiometries (n) have been determined (Table 4). These values are comparable to those observed for the albumin-binding of tryptamine ($K_a = 1.1 \times 10^4\ M^{-1}$, $n = 1$) [129], indole-3-acetic acid ($K_a = 1.7 \times 10^4\ M^{-1}$, $n = 1$) [129] and 5-hydroxyindole-3-acetic acid ($K_a = 2.0 \times 10^4\ M^{-1}$, $n = 1$) [129], and a platinum(II) polyethylene glycol complex ($K_a = 2.7 \times 10^4\ M^{-1}$, $n = 1$) [48].

To study the possible inhibition of TPase by the rhenium(I) indole complexes, a standard assay that is on the basis of the conversion of L-serine to pyruvate by the enzyme has been carried out [113]. Under our experimental conditions, at [L-serine] = 800 mM, free indole inhibits 53% of the enzyme activity, while the indole-containing complexes and their indole-free counterparts cause ca. 43–77 and 3–8% inhibition, respectively (Table 4). These results reveal that TPase can interact with these rhenium(I) indole complexes instead of their indole-free counterparts. Complexes **14b**–**17b** cause a higher extent of inhibition to the TPase-catalyzed reaction compared to complexes **14a**–**17a**, suggestive of the importance of the linker on alleviating the steric hindrance between the rhenium(I) indole complexes and the enzyme. The Michaelis constants (K_m) for the enzyme activity have been determined from plots of the linear transform of the Michaelis–Menten equation [130], and the results are listed in Table 4. Plots of v^{-1} versus [L-serine]$^{-1}$ for the TPase inhibition assays using complexes **16a**–**16c**, indole and no inhibitor are shown in Fig. 14. From the x-intercepts of the linear fits, the K_m values for the complexes have been determined to be 143–179 mM. Since the x-intercepts of all the fits are very similar, the indole-containing complexes inhibit the TPase-catalyzed conversion of L-serine to pyruvate in a non-competitive fashion.

The synthesis, characterisation, electrochemical, photophysical and protein-binding properties of four luminescent

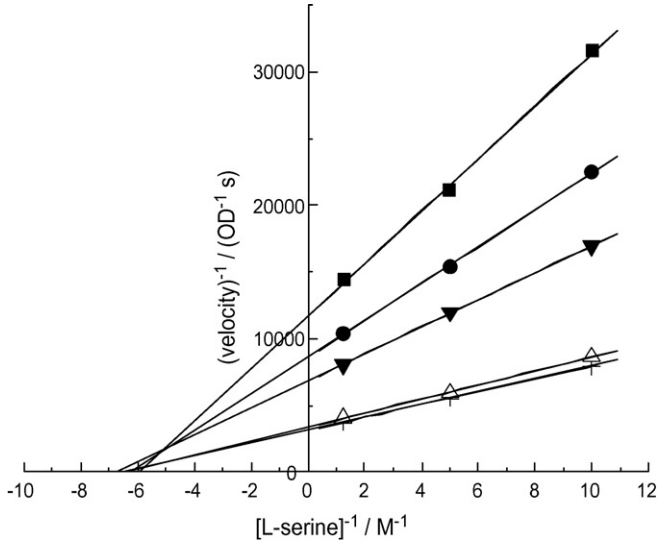

Fig. 14. Plots of v^{-1} vs. [L-serine]$^{-1}$ for the TPase inhibition assays, in which complexes **16a** (●), **16b** (■) and **16c** (△), indole (▼) or no inhibitor (+) is used. Reproduced from Ref. [123], with permission of The American Chemical Society.

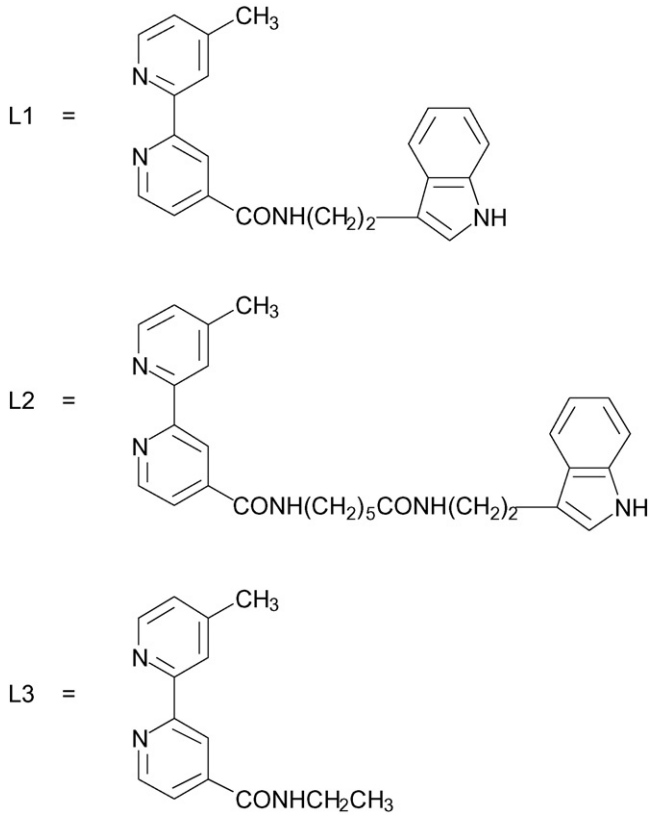

Fig. 15. Structures of the ligands L1–L3. Reproduced from Ref. [131], with permission of Elsevier.

ruthenium(II) indole complexes $[Ru(bpy)_2(L1)](PF_6)_2$ (**18**), $[Ru(bpy)_2(L2)](PF_6)_2$ (**19**), $[Ru(L1)_3](PF_6)_2$ (**18a**) and $[Ru(L2)_3](PF_6)_2$ (**19a**) (L1 = bpy-CONH-C_2H_4-indole; L2 = bpy-$CONHC_5H_{10}CONH$-C_2H_4-indole) have been reported [131]. Their indole-free counterparts $[Ru(bpy)_2(L3)](PF_6)_2$ (**20**) and $[Ru(L3)_3](PF_6)_2$ (**20a**) (L3 = bpy-CONH-Et) have also been synthesised for comparison studies [131]. The structures of the ligands L1–L3 are shown in Fig. 15. The ruthenium(II) indole complexes display intense and long-lived orange-red ^{3}MLCT ($d\pi(Ru) \rightarrow \pi^*$(bpy-indole)) luminescence upon visible-light irradiation (Table S1 of Supplementary Information). The emission properties of all the complexes are very similar and resemble those of ruthenium(II) derivatives coordinated with amide-containing bpy ligands [80,132,133].

In contrast to the rhenium(I) indole complexes described above, the indole moiety does not quench the emission of the ruihenium(II) polypyridine complexes. It appears that there is insufficient driving force for electron transfer reactions to occur because the reduction potential of indole (E^0[indole$^{+/0}$] = ca. +1.1 V versus SCE) renders the reduction of the excited ruthenium(II) polypyridine moiety ($E^0[Ru^{2+*/+}]$ = from +0.77 to +0.88 V versus SCE, estimated from E^{00} (from +2.04 to +2.08 eV) and $E^0[Ru^{2+/+}]$ (from −1.20 to −1.27 V versus SCE)) by indole thermodynamically unfavourable.

The emission quenching of all the complexes by $[Fe(CN)_6]^{4-}$ in the absence and presence of BSA in 15 mM potassium phosphate buffer pH 7.4 has been studied. The Stem–Volmer results show that the emission of all the complexes is quenched efficiently by $[Fe(CN)_6]^{4-}$ in the absence of BSA; however, in the presence of BSA (75.0 μM), the emission quenching of all the complexes becomes much less efficient (data not shown). The decrease of the quenching efficiency is much more significant for the ruthenium(II) indole complexes **18**, **19**, **18a** and **19a** than their indole-free counterparts complexes **20** and **20a**, suggestive of the binding of the indole moieties of complexes **18**, **19**, **18a** and **19a** to BSA [109–111]. The reduced quenching efficiency could be due to the immobilisation of the complexes by the protein matrix and/or the coulombic repulsion between the anionic $[Fe(CN)_6]^{4-}$ and the high negative charge of BSA, which renders the quencher ions less accessible to the protein-bound complexes.

Table 5
Relative emission intensities and lifetimes of complexes **18**–**20** and **18a**–**20a** in the absence and presence of BSA

Complex	I (τ (ns))[a,b]	I (τ (ns))[a,c]	I (τ (ns))[a,d]	I (τ (ns))[a,e]
18	1.00 (388)	1.15 (430)	1.00 (82)	2.08 (118)
19	1.00 (398)	1.07 (441)	1.00 (80)	2.58 (137)
20	1.00 (354)	1.01 (368)	1.00 (75)	1.60 (81)
18a	1.00 (418)	1.38 (618)	1.00 (113)	9.07 (511)
19a	1.00 (484)	1.19 (552)	1.00 (104)	3.90 (478)
20a	1.00 (389)	1.03 (392)	1.00 (80)	1.35 (95)

Reproduced from Ref. [131], with permission of Elsevier.
[a] Relative emission intensities and lifetimes in aerated 15 mM potassium phosphate buffer pH 7.4. [Ru] = 12.5 μM.
[b] $[[Fe(CN)_6]^{4-}]$ = 0 M, [BSA] = 0 M.
[c] $[[Fe(CN)_6]^{4-}]$ = 0 M, [BSA] = 75 μM.
[d] $[[Fe(CN)_6]^{4-}]$ = 1 mM, [BSA] = 0 μM.
[e] $[[Fe(CN)_6]^{4-}]$ = 1 mM, [BSA] = 75 μM.

The emission properties of all the complexes in the absence and presence of BSA have been studied. Unfortunately, the emission intensities and lifetimes of the ruthenium(II) complexes are only slightly increased by 1.01–1.38- and 1.01–1.48-fold, respectively) in the presence of BSA (Table 5). However, the enhancement factors are substantially improved after using $[Fe(CN)_6]^{4-}$ as a quencher. For example, the emission intensities are enhanced by 1.35–9.07-fold; and the emission lifetimes are elongated by 1.19–4.60-fold (Table 5), which indicates that ferrocyanide ions preferentially quench the free complexes compared to the BSA-bound ones. On the basis of these results, we have performed emission titrations of the complexes using BSA as the titrant and $[Fe(CN)_6]^{4-}$ (4.8 mM) as a quencher in the bulk solution. The titration curves for all the complexes are shown in Fig. 16. The ruthenium(II) indole complexes display more significant enhancement in emission intensity in the presence of BSA (2.5-, 3.1-, 19.7- and 6.3-fold for complexes **18**, **19**, **18a** and **19a** respectively, at [BSA] = 61.2 μM) (Fig. 16), owing to the less efficient quenching of the complexes by $[Fe(CN)_6]^{4-}$ after their binding to the protein. Although the indole-free complexes also show an increase in emission intensity in the presence of BSA (ca. 1.5- and 1.4-fold for complexes **20** and **20a**, respectively, at [BSA] = 61.2 μM), the increase is relatively small and is probably caused by non-specific interactions. The binding constants of the ruthenium(II) indole complexes to

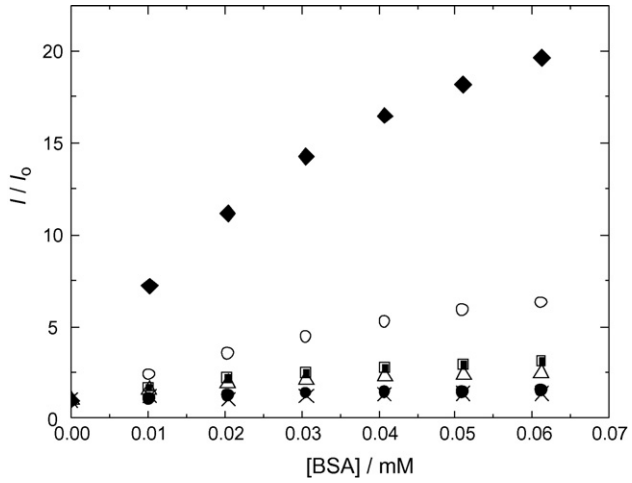

Fig. 16. Emission titration curves for the titrations of complexes **18** (△), **19** (■), **20** (●), **18a** (♦), **19a** (◯) and **20a** (×) with BSA in the presence of 4.8 mM $[Fe(CN)_6]^{4-}$. I_o and I are the emission intensities of the complexes in the absence and presence of BSA, respectively. Reproduced from Ref. [131], with permission of Elsevier.

BSA are estimated to be ca. 6.6×10^4 to $9.5 \times 10^4\ M^{-1}$ from the Scatchard analysis [134].

4. Estrogen complexes

The role of estrogen receptors (ERs) in hormone-dependent breast cancer is the focus of many clinical studies because the receptor content gives the most accurate index of the cancer [135–137]. ERs are considered to be target proteins of a number of compounds known as endocrine disrupters, some of which are environmental pollutants and hazardous to humans and animals [138,139]. The design of probes for these proteins includes radioactive estradiol derivatives such as those containing tritium [140] and technetium [141,142] because of their high detection sensitivity. Estradiol molecules labeled with biotin [143,144], organometallics [141,142,145–147], transition metal complexes [148,149] and organic fluorophores [150–152] have also been reported. However, the possibility of using luminescent organotransition metal complexes as probes for ERs has not been explored. Thus, we have designed a series of luminescent rhenium(I) estradiol complexes $[Re(N{-}N)(CO)_3(L)](CF_3SO_3)$ (N–N = phen, L = py-est (**21a**), py-C6-est (**21b**); N–N = Me_4-phen, L = py-est (**22a**), py-C6-est (**22b**); N–N = Ph_2-phen, L = py-est (**23a**), py-C6-est (**23b**)) (Fig. 17) [153]. The lipophilicity and ER-binding properties of these complexes have also been examined. Upon photoexcitation, all the complexes display intense and long-lived green to orange-yellow luminescence (Table S2 of Supplementary Information). The emission origin of the complexes is assigned to a ^{3}MLCT ($d\pi(Re) \rightarrow \pi^*(N{-}N)$) excited state [83,84]. The excited state of the py-C6-est complexes is expected to be longer-lived due to their more hydrophobic local environment associated with the longer spacer-arms. However, the py-C6-est complexes **21b**–**23b** actually display shorter excited-state lifetimes, especially in CH_2Cl_2, compared to their py-est counterparts (Table S2 of Supplementary Information). There are two possible reasons for these interesting observations. First, the electron-withdrawing ethynyl substituent on the pyridine ligand of the py-est complexes reduces the non-radiative decay rate of the complexes, as observed in other rhenium(I) polypyridine systems [154]. Second, it is possible that the longer and more flexible spacer-arms of the py-C6-est complexes facilitate their non-radiative decay, giving rise to a shorter-lived excited state.

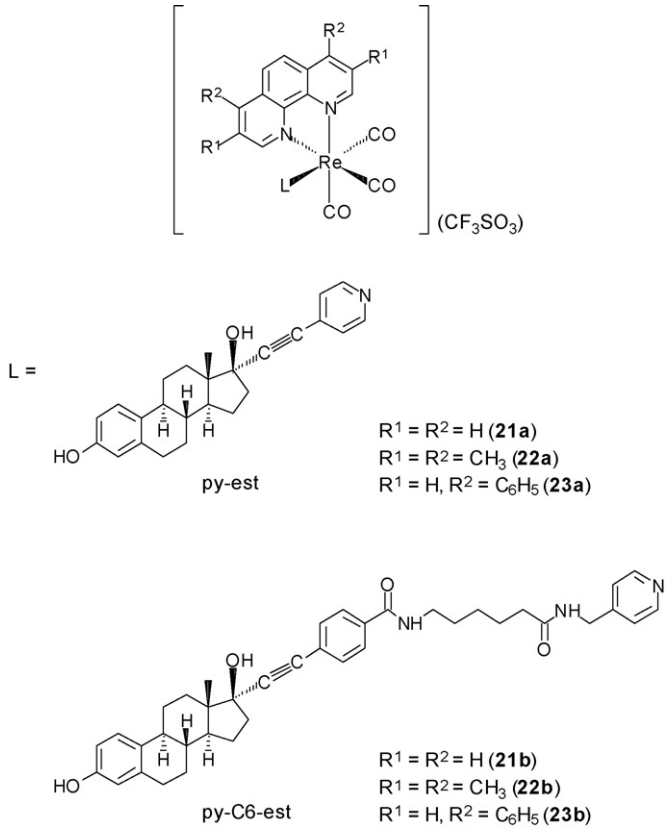

Fig. 17. Structures of complexes **21a**–**23a** and **21b**–**23b**. Reproduced from Ref. [153], with permission of The American Chemical Society.

The lipophilicity of estradiol derivatives is a good correlation with their in vivo uptake rate in fatty tissues and their non-specific binding affinity to the receptor [155]. These two factors affect the in vivo distribution and transportation of estradiol derivatives. The log $P_{o/w}$ values of these rhenium(I) estradiol complexes, determined by reversed-phase HPLC [156], are summarised in Table 6. Most of the complexes display larger log $P_{o/w}$ values than that of 17α-ethynylestradiol (3.20). We attribute these observations to the hydrophobic nature of the rhenium(I) polypyridine moieties despite their formal cationic charge. The log $P_{o/w}$ values of the complexes follow the orders: **21a** < **22a** < **23a** and **21b** < **22b** < **23b**, which is consistent with the hydrophobic character of the diimine ligands (phen < Me_4-phen < Ph_2-phen). The presence of a spacer-arm in complexes **21b**–**23b** increases the log $P_{o/w}$ values by ca. 1.3–1.5. In general, the log $P_{o/w}$ values of the py-C6-est complexes (4.34–6.48) are comparable to those of other organometallic estradiol derivatives such as 17α-$[(C{\equiv}CCH_2N(CH_3)C_2H_4N(CH_3)_2)Pt(I)_2]$-estradiol (4.02) [142], 17α-$[(C{\equiv}CC_6H_5)Cr(CO)_3]$-estradiol (5.03) [145],

Table 6
Lipophilicity (log $P_{o/w}$ values) and results of ERα-titrations of complexes **21a**–**23a** and **21b**–**23b**

Complex	log $P_{o/w}$	I/I_o[a,b]	τ_o (μs[a,c])	τ (μs[a,c])	K_a (M^{-1}[a,d])	n_H[a,e]
21a	3.07	1.08	0.53	0.53	–[f]	–[f]
21b	4.34	5.06	0.56	1.32 (14%), 0.25 (86%)	2.0×10^7	2.1
22a	3.91	0.84	1.03	1.03	–[f]	–[f]
22b	5.44	6.08	1.30	4.60 (14%), 0.70 (86%)	1.5×10^7	2.1
23a	4.99	1.38	1.24	1.31	–[f]	–[f]
23b	6.48	5.05	1.20	1.82 (14%), 0.26 (86%)	1.9×10^7	2.0

Reproduced from Ref. [153], with permission of The American Chemical Society.
[a] In aerated 50 mM potassium phosphate buffer at pH 7.4/methanol (9:1, v/v) at 298 K.
[b] I_o and I are the emission intensities of the complexes in the presence of 0 and 250 nM of ERα, respectively.
[c] τ_o and τ are the excited-state lifetimes of the complexes in the presence of 0 and 250 nM of ERα, respectively.
[d] Binding constants to ERα.
[e] Hill coefficients for the binding to ERα.
[f] These complexes do not show ERα-binding properties.

17α-[(C≡CC$_5$H$_4$)Re(CO)$_3$]-estradiol (5.31) [145], and 7α-[(C$_6$H$_{12}$SC$_2$H$_4$SCH$_3$)Re(CO)$_3$Br]-estradiol (6.29) [146].

In the presence of ERα, the emission intensities of the py-C6-est complexes **21b**–**23b** are enhanced and the emission maxima are blue-shifted. The emission spectral traces of complex **21b** are shown in Fig. 18. The emission intensities of complexes **21b**–**23b** are increased by 5.1-, 6.1- and 5.1-fold, respectively (Table 6). The emission decays are bi-exponential. The longer-lived components vary from 1.3 to 4.6 μs, which are longer than the lifetimes of the free complexes (Table 6). The increase of emission intensities and excited-state lifetimes is ascribed to the specific binding of the estradiol moieties of the complexes to ERα because the estradiol-free complexes [Re(N–N)(CO)$_3$(py)](CF$_3$SO$_3$) (N–N = phen (**21c**), Me$_4$-phen (**22c**) and Ph$_2$-phen (**23c**)) do not display similar observations. Also, when ERα which has been bound with excess estradiol is used, no significant changes are observed. The emission titration curves for complexes **21a**, **21b** and **21c** with ERα are shown in Fig. 19. The protein-induced emission enhancement and lifetime elongation of complexes **21b**–**23b** are due to the increase in hydrophobicity and rigidity of the local environment of the metal complexes. The emission intensities of the py-est complexes **21a**–**23a** do not show significant changes in the presence of ERα. It is likely that the lack of a long spacer-arm substantially reduces the protein-binding affinity of these complexes [77,82,122,123]. The binding parameters of complexes **21b**–**23b** to ERα, determined using the Hill equation [157], are summarised in Table 6. Similar to other estradiol systems [151,158], positive cooperativity is observed for the binding of the py-C6-est complexes to ERα, as evidenced by convex Scatchard plots and that the n_H values are >1. The binding constants of these complexes are smaller than that of unmodified estradiol ($K_a = 5 \times 10^9\ M^{-1}$) [159]. The lower binding affinity may be a result of the bulkiness of rhenium(I) polypyridine moieties, which increases the steric hindrance between the complexes and the receptor. Nevertheless, these binding constants are comparable or larger than those of other related estradiol systems such as 17α-[(L)Re(CO)$_3$]-estradiol (L = 4′,4′-bis(ethanethio)-4′-

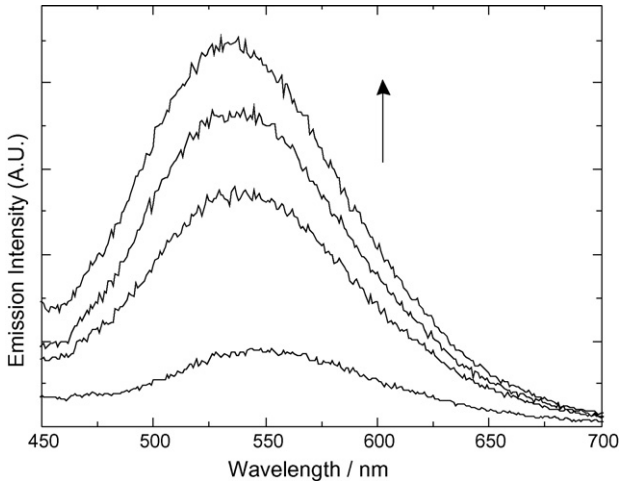

Fig. 18. Emission spectral traces of complex **21b** in 50 mM potassium phosphate buffer pH 7.4/methanol (9:1, v/v) at 298 K in the presence of 0, 50, 100 and 200 nM ERα. Reproduced from Ref. [153], with permission of The American Chemical Society.

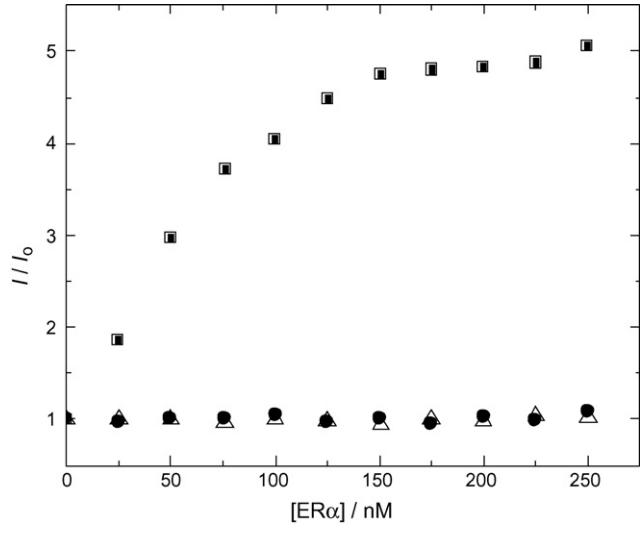

Fig. 19. Emission titration curves for complexes **21a** (●), **21b** (■) and **21c** (△) with ERα. The emission intensities of the complexes are monitored at ca. 548 nm. Reproduced from Ref. [153], with permission of The American Chemical Society.

carboxy-butyn-1′-yl, 6′,6′-bis(ethanethio)-6′-carboxy-hexyn-1′-yl; $K_a = 1.3 \times 10^7$ and $1.1 \times 10^7\ M^{-1}$, respectively) [141] and 17α-[(C≡CCH$_2$N(CH$_3$)C$_2$H$_4$N(CH$_3$)$_2$)Pt(X)]-estradiol (X = diiodide, malonato; $K_a = 1.0 \times 10^7$ and $2.5 \times 10^6\ M^{-1}$, respectively) [142].

5. Concluding remarks

Many luminescent transition metal complexes possess variable coordination geometry and rich photophysical and electrochemical properties that can be exploited in understanding biological systems. It is evident that luminescent rhenium(I), iridium(III) and ruthenium(II) polypyridine complexes can act as probes for various proteins. Given the high environment-sensitive emission behaviour of these complexes, and the use of other entities such as quenchers, macromolecular architectures such as hydrophobic micellar and dendritic systems, we anticipate that luminescent metal complexes can further contribute to the design of new biological probes and analytical assays.

Acknowledgements

We thank the Hong Kong Research Grants Council (Project Numbers CityU 101603, CityU 101704 and CityU 101605) and the City University of Hong Kong (Project Numbers 7001632, 7001456, 7001985 and 7001283) for financial support. K.H.-K. T., K.-S. S., C.-K. C., K.Y. Z., W.-K. H. and J.S.-Y. L. acknowledge the receipt of a Postgraduate Studentship and a Research Tuition Scholarship, both administered by the City University of Hong Kong. K.K.-W. L. thanks the Faculty of Science and Engineering for financial support (Young/Junior Scholars Scheme).

Appendix A. Supplementary data

Supplementary data associated with this article can be found, in the online version, at doi:10.1016/j.ccr.2006.12.005.

References

[1] V. Balzani, F. Scandola, Supramolecular Photochemistry, Ellis Horwood, New York, 1990.
[2] K. Kalyanasundaram, Photochemistry of Polypyridine and Porphyrin Complexes, Academic Press, San Diego, 1992.
[3] D.M. Roundhill, Photochemistry and Photophysics of Metal Complexes, Plenum Press, New York, 1994.
[4] V. Balzani, A. Juris, M. Venturi, S. Campagna, S. Serroni, Chem. Soc. Rev. 96 (1996) 759.
[5] A. Vogler, H. Kunkely, Top. Curr. Chem. 213 (2001) 143.
[6] V. Balzani, M. Venturi, A. Credi, Molecular Devices and Machine, Wiley–VCH, Weinheim, 2003.
[7] G.B. Dreyer, P.B. Dervan, Proc. Natl. Acad. Sci. U.S.A. 82 (1985) 968.
[8] T. Le Doan, L. Perrouault, M. Chassignol, N.T. Thuong, C. Helene, Nucleic Acids Res. 15 (1987) 8643.
[9] J. Telser, K.A. Cruickshank, K.S. Schanze, T.L. Netzel, J. Am. Chem. Soc. 111 (1989) 7221.
[10] F.D. Lewis, S.A. Helvoigt, R.L. Letsinger, Chem. Commun. (1999) 327.
[11] S.I. Khan, A.E. Beilstein, M.T. Tierney, M. Sykora, M.W. Grinstaff, Inorg. Chem. 38 (1999) 5999.
[12] J.J. Rack, E.S. Krider, T.J. Meade, J. Am. Chem. Soc. 122 (2000) 6287.
[13] D.J. Hurley, Y. Tor, J. Am. Chem. Soc. 124 (2002) 3749.
[14] D.J. Hurley, Y. Tor, J. Am. Chem. Soc. 124 (2002) 13231.
[15] Y. Jenkins, J.K. Barton, J. Am. Chem. Soc. 114 (1992) 8736.
[16] I. Ortmans, S. Content, N. Boutonnet, A. Kirsch-De Mesmaeker, W. Bannwarth, J.F. Constant, E. Defrancq, J. Lhomme, Chem. Eur. J. 5 (1999) 2712.
[17] R.E. Holmlin, R.T. Tong, J.K. Barton, J. Am. Chem. Soc. 120 (1998) 9724.
[18] K.K.-W. Lo, D.C.-M. Ng, W.-K. Hui, K.-K. Cheung, J. Chem. Soc., Dalton Trans. (2001) 2634.
[19] K.K.-W. Lo, W.-K. Hui, D.C.-M. Ng, K.-K. Cheung, Inorg. Chem. 41 (2002) 40.
[20] L. Wei, J. Babich, W.C. Eckelman, J. Zubieta, Inorg. Chem. 44 (2005) 2198.
[21] K.K.-W. Lo, D.C.-M. Ng, C.-K. Chung, Organometallics 20 (2001) 4999.
[22] D.R. McMillin, K.M. McNett, Chem. Rev. 98 (1998) 1201.
[23] K.E. Erkkila, D.T. Odom, J.K. Barton, Chem. Rev. 99 (1999) 2777.
[24] C. Metcalfe, J.A. Thomas, Chem. Soc. Rev. 32 (2003) 215.
[25] F. Pierard, A. Kirsch-De Mesmaeker, Inorg. Chem. Commun. 9 (2006) 111.
[26] J.R. Winkler, D.G. Nocera, K.M. Yocom, E. Bordignon, H.B. Gray, J. Am. Chem. Soc. 104 (1982) 5798.
[27] R. Langen, I.J. Chang, J.P. Germanas, J.H. Richards, J.R. Winkler, H.B. Gray, Science 268 (1995) 1733.
[28] J.J. Regan, A.J. Di Bilio, R. Langen, L.K. Skov, J.R. Winkler, H.B. Gray, J.N. Onuchic, Chem. Biol. 2 (1995) 489.
[29] W.B. Connick, A.J. Di Bilio, M.G. Hill, J.R. Winkler, H.B. Gray, Inorg. Chim. Acta 240 (1995) 169.
[30] A.J. Di Bilio, B.R. Crane, W.A. Wehbi, C.N. Kiser, M.M. Abu-Omar, R.M. Carlos, J.H. Richards, J.R. Winkler, H.B. Gray, J. Am. Chem. Soc. 123 (2001) 3181.
[31] J.E. Miller, A.J. Di Bilio, W.A. Wehbi, M.T. Green, A.K. Museth, J.H. Richards, J.R. Winkler, H.B. Gray, Biochim. Biophys. Acta 1655 (2004) 59.
[32] L.P. Pan, B. Durham, J. Wolinska, F. Millett, Biochemistry 27 (1988) 7180.
[33] H. Szmacinski, E. Terpetschnig, J.R. Lakowicz, Biophys. Chem. 62 (1996) 109.
[34] X.-Q. Guo, F.N. Castellano, L. Li, H. Szmacinski, J.R. Lakowicz, J. Sipior, Anal. Biochem. 254 (1997) 179.
[35] E. Terpetschnig, H. Szmacinski, J.R. Lakowicz, Anal. Biochem. 240 (1996) 54.
[36] Z. Murtaza, P. Herman, J.R. Lakowicz, Biophys. Chem. 80 (1999) 143.
[37] E.M. Ryan, R. O'Kennedy, M.M. Feeney, J.M. Kelly, J.G. Vos, Bioconjugate Chem. 3 (1992) 285.
[38] K.K.-W. Lo, C.-K. Chung, T.K.-M. Lee, L.-H. Lui, K.H.-K. Tsang, N. Zhu, Inorg. Chem. 42 (2003) 6886.
[39] K.M.-C. Wong, W.S. Tang, B.W.-K. Chu, N. Zhu, V.W.-W. Yam, Organometallics 23 (2004) 3459.
[40] K.K.-W. Lo, C.-K. Chung, N. Zhu, Chem. Eur. J. 9 (2003) 475.
[41] K.K.-W. Lo, C.-K. Li, K.-W. Lau, N. Zhu, Dalton Trans. (2003) 4682.
[42] K.K.-W. Lo, J.S.-W. Chan, C.-K. Chung, V.W.-H. Tsang, N. Zhu, Inorg. Chim. Acta 357 (2004) 3109.
[43] G.T. Hermanson, Bioconjugate Techniques, Academic Press, San Diego, 1996.
[44] S.R. Banerjee, P. Schaffer, J.W. Babich, J.F. Valliant, J. Zubieta, Dalton Trans. (2005) 3886.
[45] J.D. Dattelbaum, O.O. Abugo, J.R. Lakowicz, Bioconjugate Chem. 11 (2000) 533.
[46] A.R. Dunn, I.J. Dmochowski, J.R. Winkler, H.B. Gray, J. Am. Chem. Soc. 125 (2003) 12450.
[47] W. Belliston-Bittner, A.R. Dunn, Y.H.L. Nguyen, D.J. Stuehr, J.R. Winkler, H.B. Gray, J. Am. Chem. Soc. 127 (2005) 15907.
[48] C.-M. Che, J.-L. Zhang, L.-R. Lin, Chem. Commun. (2002) 2556.
[49] K.K.-W. Lo, W.-K. Hui, C.-K. Chung, K.H.-K. Tsang, T.K.-M. Lee, C.-K. Li, J.S.-Y. Lau, D.C.-M. Ng, Coord. Chem. Rev. 250 (2006) 1724.
[50] N.M. Green, Adv. Protein Chem. 29 (1975) 85.
[51] N.M. Green, Methods Enzymol. 184 (1990) 51.

[52] O. Livnah, E.A. Bayer, M. Wilchek, J.L. Sussman, Proc. Natl. Acad. Sci. U.S.A. 90 (1993) 5076.
[53] L. Pugliese, A. Coda, M. Malcovati, M. Bolognesi, J. Mol. Biol. 231 (1993) 698.
[54] S. Repo, T.A. Paidanius, V.P. Hytönen, T.K.M. Nyholm, K.K. Halling, J. Huuskonen, T. Pentikäinen, K. Rissanen, J.P. Slotte, T.T. Airenne, T.A. Salminen, M.S. Kulomaa, M.S. Johnson, Chem. Biol. 13 (2006) 1029.
[55] M. Wilchek, E.A. Bayer, Methods Enzymol. 184 (1990) 123.
[56] D.M. Mock, P. Horowitz, Methods Enzymol. 184 (1990) 234.
[57] M. Wilchek, E.A. Bayer, Anal. Biochem. 177 (1988) 1.
[58] G. Kada, H. Falk, H.J. Gruber, Biochim. Biophys. Acta 1427 (1999) 33.
[59] G. Kada, K. Kaiser, H. Falk, H.J. Gruber, Biochim. Biophys. Acta 1427 (1999) 44.
[60] X. Song, B.I. Swanson, Anal. Chim. Acta 442 (2001) 79.
[61] H.J. Gruber, M. Marek, H. Schindler, K. Kaiser, Bioconjugate Chem. 8 (1997) 552.
[62] J.R. Lakowicz, Principles of Fluorescence Spectroscopy, second ed., Kluwer Academic/Plenum Publishers, New York, 1999, p. 373.
[63] M. Salmain, N. Fischer-Durand, L. Cavalier, B. Rudolf, J. Zakrzewski, G. Jaouen, Bioconjugate Chem. 13 (2002) 693.
[64] A. Anne, Tetrahedron Lett. 39 (2002) 693.
[65] N. Haddour, C. Gondran, S. Cosnier, Chem. Commun. (2004) 324.
[66] X. Zhou, J. Shearer, S.E. Rokita, J. Am. Chem. Soc. 122 (2000) 9046.
[67] A. Loosli, U.E. Rusbandi, J. Gradinaru, K. Bernauer, C.W. Schlaepfer, M. Meyer, S. Mazurek, M. Novic, T.R. Ward, Inorg. Chem. 45 (2006) 660.
[68] M. Slim, H.F. Sleiman, Bioconjugate Chem. 15 (2004) 949.
[69] C. Letondor, N. Humbert, T.R. Ward, Proc. Natl. Acad. Sci. U.S.A. 102 (2005) 4683.
[70] H.B. Gray, J.R. Winkler, Annu. Rev. Biochem. 65 (1996) 537.
[71] S.M. Cohen, S.J. Lippard, Prog. Nucleic Acid Res. 67 (2001) 93.
[72] A.E. Beilstein, M.T. Tierney, M.W. Gristaff, Comments Inorg. Chem. 22 (2000) 105.
[73] E. Terpetschnig, H. Szmacinski, J.R. Lakowicz, Methods Enzymol. 278 (1997) 295.
[74] D.M. Perrin, A. Mazumder, D.S. Sigman, Prog. Nucleic Acid Res. 52 (1996) 123.
[75] J.R. Winkler, H.B. Gray, Chem. Rev. 92 (1992) 369.
[76] K.K.-W. Lo, W.-K. Hui, D.C.-M. Ng, J. Am. Chem. Soc. 124 (2002) 9344.
[77] K.K.-W. Lo, W.-K. Hui, Inorg. Chem. 44 (2005) 1992.
[78] K.K.-W. Lo, J.S.-W. Chan, L.-H. Lui, C.-K. Chung, Organometallics 23 (2004) 3018.
[79] K.K.-W. Lo, C.-K. Li, J.S.-Y. Lau, Organometallics 24 (2005) 4594.
[80] K.K.-W. Lo, T.K-M. Lee, Inorg. Chem. 43 (2004) 5275.
[81] K.A. O'Donoghue, J.M. Kelly, P.E. Kruger, Dalton Trans. (2004) 13.
[82] K.K.-W. Lo, K.H.-K. Tsang, K.-S. Sze, Inorg. Chem. 45 (2006) 1714.
[83] A.J. Lees, Chem. Rev. 4 (1987) 711.
[84] A. Vlček Jr., Coord. Chem. Rev. 230 (2002) 225.
[85] K.S. Schanze, D.B. MacQueen, T.A. Perkins, L.A. Cabana, Coord. Chem. Rev. 122 (1993) 63.
[86] N.B. Thornton, K.S. Schanze, Inorg. Chem. 32 (1993) 4994.
[87] N.B. Thornton, K.S. Schanze, New J. Chem. 20 (1996) 791.
[88] A.P. Wilde, K.A. King, R.J. Watts, J. Phys. Chem. 95 (1991) 629.
[89] E. Baranoff, I.M. Dixon, J.-P. Collin, J.-P. Sauvage, B. Ventura, L. Flamigni, Inorg. Chem. 43 (2004) 3057.
[90] S. Lamansky, P. Djurovich, D. Murphy, F. Abdel-Razzaq, H.-E. Lee, C. Adachi, P.E. Burrows, S.R. Forrest, M.E. Thompson, J. Am. Chem. Soc. 123 (2001) 4304.
[91] S. Serroni, A. Juris, S. Campagna, M. Venturi, G. Denti, V. Balzani, J. Am. Chem. Soc. 116 (1994) 9086.
[92] I. Ortmans, P. Didier, A. Kirsch-De Mesmaeker, Inorg. Chem. 34 (1995) 3695.
[93] M. Licini, J.A.G. Williams, Chem. Commun. (1999) 1943.
[94] T. Yutaka, S. Obara, S. Ogawa, K. Nozaki, N. Ikeda, T. Ohno, Y. Ishii, K. Sakai, M. Haga, Inorg. Chem. 44 (2005) 4737.
[95] K.K.-W. Lo, C.-K. Chung, N. Zhu, Chem. Eur. J. 12 (2006) 1500.
[96] R.M. Hartshorn, J.K. Barton, J. Am. Chem. Soc. 114 (1992) 5919.
[97] C.J. Murphy, M.R. Arkin, Y. Jenkins, N.D. Ghatlia, S.H. Bossmann, R.E. Holmlin, J.K. Barton, Science 262 (1993) 1025.
[98] K.K.-W. Lo, T.K-M. Lee, Inorg. Chim. Acta 360 (2007) 293.
[99] A. Delgadillo, P. Romo, A.M. Leiva, B. Loeb, Helv. Chim. Acta 86 (2003) 2110.
[100] K. Kalyanasundaram, Coord. Chem. Rev. 46 (1982) 159.
[101] A. Juris, V. Balzani, F. Barigelletti, S. Campagna, P. Belser, A. von Zelewsky, Coord. Chem. Rev. 84 (1988) 85.
[102] K. Shinozaki, T. Shinoyama, Chem. Phys. Lett. 417 (2006) 111.
[103] D.V. Kozlov, F.N. Castellano, J. Phys. Chem. A 108 (2004) 10619.
[104] M.K. Brennaman, J.H. Alstrum-Acevedo, C.N. Fleming, P. Jang, T.J. Meyer, J.M. Papanikolas, J. Am. Chem. Soc. 124 (2002) 15094.
[105] M.K. Brennaman, T.J. Meyer, J.M. Papanikolas, J. Phys. Chem. A 108 (2004) 9938.
[106] T. Ishida, M. Hamada, M. Inoue, A. Wakahara, Chem. Pharm. Bull. 38 (1990) 851.
[107] B. Bartel, Annu. Rev. Plant Physiol. 48 (1997) 51.
[108] J.D. Lang Jr., M. Figueroa, P. Chumley, M. Asian, J. Hurt, M.M. Tarpey, B. Alvarez, R. Radi, B.A. Freeman, Anesthesiology 100 (2004) 51.
[109] D.C. Carter, J.X. Ho, Adv. Protein Chem. 45 (1994) 153.
[110] F.A. de Wolf, G.M. Brett, Pharmacol. Rev. 52 (2000) 207.
[111] K.N. Houk, A.G. Leach, S.P. Kim, X. Zhang, Angew. Chem. Int. Ed. 42 (2003) 4872.
[112] W.A. Newton, Y. Morino, E.E. Snell, J. Biol. Chem. 240 (1965) 1211.
[113] Y. Morino, E.E. Snell, J. Biol. Chem. 242 (1967) 2793.
[114] J. Bilang, H. Macdonald, P.J. King, A. Sturm, Plant Physiol. 102 (1993) 29.
[115] R. Zettl, J. Schell, K. Palme, Proc. Natl. Acad. Sci. U.S.A. 91 (1994) 689.
[116] A. Mazzini, P. Cavatorat, M. Iori, R. Favilla, G. Sartor, Biophys. Chem. 42 (1992) 101.
[117] M. Shinitzky, E. Katchalski, V. Grisaro, N. Sharon, Arch. Biochem. Biophys. 116 (1966) 332.
[118] I.D.A. Swan, J. Mol. Biol. 65 (1972) 59.
[119] E. Dolušić, M. Kowalczyk, V. Magnus, G. Sandberg, J. Normanly, Bioconjugate Chem. 12 (2001) 152.
[120] N.E. Schore, N.J. Turro, J. Am. Chem. Soc. 97 (1975) 2488.
[121] P.K. Bowyer, D.St.C. Black, D.C. Craig, A.D. Rae, A.C. Willis, J. Chem. Soc. Dalton Trans. (2001) 1948.
[122] K.K.-W. Lo, K.H.-K. Tsang, W.-K. Hui, N. Zhu, Chem. Commun. 44 (2003) 2704.
[123] K.K.-W. Lo, K.H.-K. Tsang, W.-K. Hui, N. Zhu, Inorg. Chem. 44 (2005) 6100.
[124] R. Klein, I. Tatischeff, M. Bazin, R. Santua, J. Phys. Chem. 85 (1981) 670.
[125] P. Chen, R. Duesing, D.K. Graff, T.J. Meyer, J. Phys. Chem. 95 (1991) 5850.
[126] L.A. Lucia, K. Abboud, K.S. Schanze, Inorg. Chem. 36 (1997) 6224.
[127] K. Kasama, A. Takematsu, S. Aral, J. Phys. Chem. 86 (1982) 2420.
[128] S.V. Jovanovic, S. Steenken, J. Phys. Chem. 96 (1992) 6674.
[129] N. Okabe, K. Adachi, Chem. Pharm. Bull. 40 (1992) 499.
[130] G. Atkins, I.A. Nimmo, Biochem. J. 135 (1973) 779.
[131] K.K.-W. Lo, T.K.-M. Lee, K.Y. Zhang, Inorg. Chim. Acta 359 (2006) 1845.
[132] S.L. Mecklenburg, B.M. Peek, J.R. Schoonover, D.G. McCafferty, C.G. Wall, B.W. Erickson, T.J. Meyer, J. Am. Chem. Soc. 115 (1993) 5479.
[133] I.M.M.D. Carvalho, I.D.S. Moreira, M.H. Gehlen, Inorg. Chem. 42 (2003) 1525.
[134] G. Scatchard, I.H. Scheinberg, S.H. Armstrong, J. Am. Chem. Soc. 72 (1950) 535.
[135] W.L. McGuire, Proc. Soc. Exp. Biol. Med. 162 (1979) 22.
[136] K.B. Horwitz, J. Steroid Biochem. 27 (1987) 447.
[137] G.A. Gelbfish, A.L. Davison, S. Kopel, B. Schreibman, J.S. Gelbfish, G.A. Degenshein, B.L. Herz, J.N. Cunningham, Ann. Surg. 207 (1988) 75.
[138] T. Colborn, F.S. vom Saal, A.M. Soto, Environ. Health Perspect. 101 (1993) 378.
[139] T. Colborn, Environ. Health Perspect. 103 (1995) 135.
[140] P.G. Davis, B.S. McEwen, D.W. Pfaff, Endocrinology 104 (1979) 898.

[141] L.G. Luyt, H.M. Bigott, M.J. Welch, J.A. Katzenellenbogen, Bioorg. Med. Chem. 11 (2003) 4977.
[142] C. Cassino, E. Gabano, M. Ravera, G. Cravotto, G. Palmisano, A. Vessières, G. Jaouen, S. Mundwiler, R. Alberto, D. Osella, Inorg. Chim. Acta 357 (2004) 2157.
[143] A. Mares, J. DeBoever, G. Stans, E. Bosmans, F. Kohen, J. Immunol. Methods 183 (1995) 211.
[144] H. Hauptmann, B. Paulus, T. Kaiser, P.B. Luppa, Bioconjugate Chem. 11 (2000) 537.
[145] S. Top, H. El Hafa, A. Vessières, J. Quivy, J. Vaissermann, D.W. Hughes, M.J. McGlinchey, J.-P. Momon, E. Thoreau, G. Jaouen, J. Am. Chem. Soc. 117 (1995) 8372.
[146] M.B. Skaddan, F.R. Wüst, J.A. Katzenellenbogen, J. Org. Chem. 64 (1999) 8108.
[147] A. Vessières, S. Top, A.A. Ismail, I.S. Butler, M. Louer, G. Jaouen, Biochemistry 27 (1988) 6659.
[148] E. Gabano, C. Cassino, S. Bonetti, C. Prandi, D. Conangelo, A. Chiglia, D. Osella, Org. Biomol. Chem. 3 (2005) 3531.
[149] V. Gagnon, M.-E. St-Germain, C. Descôteaux, J. Provencher-Mandeville, S. Parent, S.K. Mandal, E. Asselin, G. Bérubé, Bioorg. Med. Chem. Lett. 14 (2004) 5919.
[150] M. Adamczyk, Y.-Y. Chen, J.C. Gebler, D.D. Johnson, P.G. Mattingly, J.A. Moore, R.E. Reddy, J. Wu, Z. Yu, Steroids 65 (2000) 295.
[151] K. Ohno, T. Fukushima, T. Santa, N. Waizumi, H. Tokuyama, M. Maeda, K. Imai, Anal. Chem. 74 (2002) 4391.
[152] L. Kokko, K. Sandberg, T. Lövgren, T. Sunkka, Anal. Chim. Acta 503 (2004) 155.
[153] K.K.-W. Lo, K.H.-K. Tsang, N. Zhu, Organometallics 25 (2006) 3220.
[154] L. Sacksteder, A.P. Zipp, E.A. Brown, J. Streich, J.N. Demas, B.A. DeGraff, Inorg. Chem. 29 (1990) 4335.
[155] H.F. VanBrocklin, A. Liu, M.J. Welch, J.P. O'Neil, J.A. Katzenellenbogen, Steroids 59 (1994) 34.
[156] D.J. Minick, J.H. Frenz, M.A. Patrick, D.A. Brent, J. Med. Chem. 31 (1988) 1923.
[157] Y. Yamada, K. Matsuura, K. Kobayashi, Bioorg. Med. Chem. 13 (2005) 1913.
[158] J.A. Schwartz, D.F. Skafar, Biochemistry 32 (1993) 10109.
[159] J.A. Katzenellenbogen, H.J. Johnson Jr., H.N. Meyers, Biochemistry 12 (1973) 4085.